# Prolonged illumination up-regulates arrestin and two GCAPs: a novel mechanism for light adaptation

Thesis submitted for the degree of

*"Doctor Philosophiæ"*

S.I.S.S.A. - I.S.A.S.
Neurobiology Sector

20 November 2008

CANDIDATE

Paolo Codega

SUPERVISOR

Prof. Vincent Torre

*"we all shine on, like the moon and the stars and the sun"*
*(John Lennon)*

# Declaration

The work described in this thesis was carried out at the International School for Advanced Studies, Trieste, between November 2004 and August 2008 with the exception of the microarray screening that I performed in May 2006 at *Gurdon Institute (Cambridge, UK)* under the supervision of Prof. Rick Livesey and the in vivo ERG recordings, performed by Luca Della Santina e Claudia Gargini at *Università di Pisa.*

The work described in this thesis is included in:

***Paolo Codega**, Luca Della Santina, Claudia Gargini, Diana E. Bedolla, Tatiana Subkhankulova, Frederick J. Livesey, Luigi Cervetto and Vincent Torre.*
Prolonged illumination up-regulates arrestin and two GCAPs: a novel mechanism for light adaptation
*under review*

# Abstract

In vertebrate photoreceptors, light adaptation is mediated by multiple mechanisms but the genomic contribution to these mechanisms has never been studied before. Therefore, we have investigated changes of gene expression using microarrays and real-time PCR in isolated photoreceptors, in cultured isolated retinas and in acutely isolated retinas. In all these three preparations after 2 hours of exposure to a steady light, we observed an up-regulation of almost two-fold of three genes *Sag*, *Guca1a* and *Guca1b*, coding for proteins known to play a major role in phototransduction: arrestin and guanylate cyclase activators 1 and 2. This up-regulation has intensity-dependent characteristics and leads to an increase in the related protein content. Indeed, after three hours of light exposure, the protein concentration of arrestin and GCAPs increases by about 40-50%. The up-regulation of these proteins in light conditions is expected to reactivate the photocurrent and thus to mediate a late phase of light adaptation. Functional *in vivo* electroretinographic tests show in fact that a partial recovery of the dark current occurs 1-2 hours after prolonged illumination with a steady light that initially causes a substantial suppression of the photoresponse. These observations demonstrate that a prolonged illumination results in the up-regulation of genes coding for proteins involved in the phototransduction signaling cascade, possibly underlying a novel component of light adaptation occurring 1-2 hours after the onset of a steady light.

# Contents

# List of Figures

## LIST OF FIGURES

| | |
|---|---|
| AC | amacrine cell |
| BC | bipolar cell |
| CNG channel | cyclic nucleotide gated channel |
| cGMP | guanosine 3'5'-cyclic monophosphate |
| DAPI | 4',6-diamidino-2-phenylindole |
| G protein | GTP-binding protein |
| GABA | $\gamma$-aminobutyric acid |
| GCAP | guanylate cyclase activating protein |
| GCL | ganglion cell layer |
| Gnat-1 | gene coding for transducin $\alpha$-subunit |
| GPCR | G-protein coupled receptor |
| GTP | guanosine 5'-triphosphate |
| Guca1a | gene coding for GCAP1 |
| Guca1b | gene coding for GCAP2 |
| HC | horizontal cell |
| INL | inner nuclear layer |
| IPL | inner plexiform layer |
| ONL | outer nuclear layer |
| OPL | outer plexiform layer |
| PDE | cGMP-specific phosphodiesterase |
| PDE6b | gene coding for cGMP-specific phosphodiesterase $\beta$-subunit |
| $R^*$ | metarhodopsin II, the active form of rhodopsin |
| RGC | retinal ganglion cell |
| RIS | rod inner segment |
| ROS | rod outer segment |
| Sag | retinal S-antigen |
| ST | synaptic terminal |

# 1

# Introduction

## 1.1 The structure of the eye and of the retina

Most of our perception of the world and our memories of it are based on sight and the eyes are the tools deputed to this function. The vertebrate eye is a complex and very specialized sense organ and its main components are:

- **the cornea,** a transparent external surface that is the first and most powerful lens of the optical system of the eye;
- **the crystalline lens,** a biconvex transparent structure that allows us, by changing its shape, to change the focal distance of the eye;
- **the pupil,** an aperture that allows light to enter the eye;
- **the iris,** a pigmented circular muscle that controls, by reducing or increasing the size of the pupil, the amount of light entering the eye;
- **the anterior chamber** (between cornea and iris), **the posterior chamber** (between iris and lens) and **the vitreous chamber** (between the lens and the retina). The first two chambers are filled with aqueous humor whereas the vitreous chamber is filled with a more viscous fluid, the vitreous humor;
- **the retina,** the light sensitive part inside the inner layer of the eye that receives light and transforms it into signals which are transmitted through the optic nerve to the brain;

- **the sclera,** which forms part of the supporting wall of the eyeball. The sclera is continuous with the cornea and with the dura of the central nervous system.

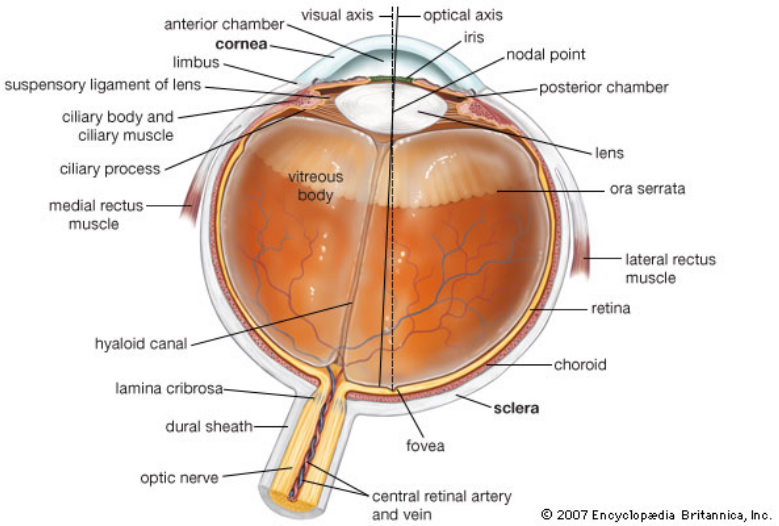


**Figure 1.1: The human eye** - a schematic representation of eye structure *(from Encyclopædia Britannica)*

Although all parts of the eye are important for perceiving light stimuli and forming a good image, the most crucial element in the visual system is the retina. Understanding the organization of the vertebrate retina has been the goal of many talented visual scientists over the past 100 years. Cajal's (1892) anatomic descriptions of the retinal cell types, together with an early understanding of photochemistry and psychophysical studies, were instrumental to understand how the retina might be organized and functioning.
The retina is part of the central nervous system and is organized as a circuit of neurons (its name derives from the Latin word *Rete*: net). In particular, the different types of neurons present in the retina are:

- **photoreceptors,** which are the photosensitive cells that are capable of detecting photons and of converting the light signal in an electrophysiological response;
- **horizontal cells,** which are the laterally interconnecting neurons that help integrate and regulate the input from multiple photoreceptor cells;
- **bipolar cells,** that transmit signals from the photoreceptors to the ganglion cells;

- **amacrine cells,** which are interneurons that regulate interactions between bipolar and ganglion cells;
- **ganglion cells,** that collect visual information from the other neurons of the retina and transmit it to several regions of the thalamus, hypothalamus, and mesencephalon, or midbrain.

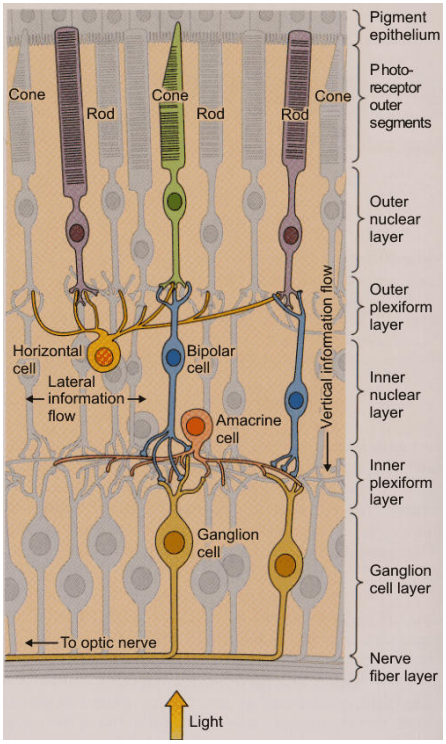


**Figure 1.2: Schematics of the retina cellular structure** - The figure shows the different cell types present in the vertebrate retina *(from Purves et al., "Neuroscience", Sinauer Associates Inc. Publishers)*

### 1.1.1 Photoreceptor cells

The great biological importance of photoreceptors is that they convert light (electromagnetic radiation) into the starting point in a chain of biological processes. More specifically, the photoreceptor absorbs photons, and through a well defined and complex biochemical pathway, known as *phototransduction*, transforms this signal into a change in its membrane potential.

In vertebrates, photoreceptors are divided into two classes: rods and cones and they are both involved in the image-forming vision. Rods and cones have major functional differences.

The cone system is devoted to detect colors and is optimized to work in bright light, whereas the rod system is responsible for the monochromatic vision occuring in low light ambient. In humans, there are three different types of cones, responding respectively to short (blue), medium (green) and long (red) light wavelenghts (84), whereas mice have only two type of cones, one responding in the ultra-violet region of the vision spectrum and the other sensitive to the green light (43).

Rods and cones are a very specialized class of neurons and they have a peculiar shape, aimed at performing one main function: *catching the photons.* The cellular compartiments (see Figure 1.3) can be subdivided into:

- **outer segment (OS),** located at the distal surface of the retina, containing all the phototransduction machinery;
- **inner segment (IS),** where most of the biosynthetic processes take place;
- **nuclear body (N),** located in the outer nuclear layer, containing the nucleus;
- **synaptic terminal (ST),** the region of contact with the photoreceptor's target cells.

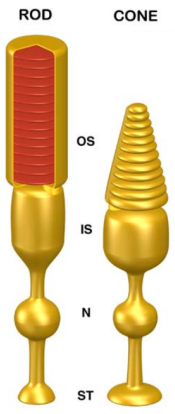


**Figure 1.3: Rods and cones share similar structures** - *(modified from Burns and Arshavsky, 2005)*

The outer segment is the specialized light-sensing organelle and it is the site where the phototransduction process takes place. The rod OS consists of a plasma membrane that encloses a stack of about 1000 closely spaced membranous discs. This arrangement dramatically increases the surface area of the membrane in these cells. OSs are continuously renewed throughout their lifetime (132). New discs are assembled at the base of the OS, they mature during migration to the distal tip where aged discs are shedded and degradated, engulfed by retinal pigment epithelial (RPE) cells. The OS discs are densely packed with rhodopsin, the proteic light detector.

From an electrophysiological point of view, photoreceptors act in the opposite way compared to other neurons. As shown in Figure 1.4, they are depolarized when the phototransduction machinery is not activated (in the dark), whereas they hyperpolarize as a consequence of photoactivation (in the light). In the dark, two currents predominate in a photoreceptor. An inward current flows through cGMP-gated channels (CNG channels), while an outward $K^+$ current flows through non-gated $K^+$-selective channels. The outward current carried by the $K^+$ channels tends to hyperpolarize the photoreceptor towards the equilibrium potential for $K^+$ (about -70 mV). On the contrary, the inward current tends to depolarize the cell. A steady intracellular concentrations of $Na^+$ and $K^+$ is maintained by $Na^+$-$K^+$ pumps, which pump $Na^+$ out and pump $K^+$ in.

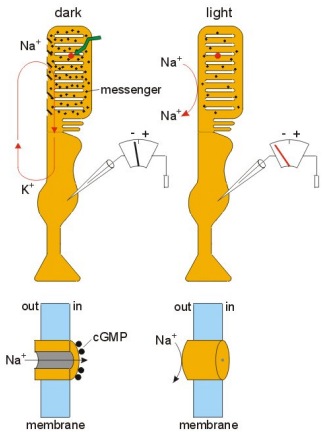


**Figure 1.4: The dark current** - The inward current that flows into a photoreceptor is supressed by bright light, hyperpolarizing the cell *(from www.fz-juelich.de/ind/ind-1/Photoreception)*

In the dark, the cytoplasmic concentration of cGMP is relatively high, maintaining in this way the CNG channels in a open state and allowing a steady inward current, called the dark current. As a result, in the dark the photoreceptor membrane potential is around -40 mV. When light reduces the level of cGMP, closing the CNG channels, the inward current that flows through these channels is reduced and the cell becomes hyperpolarized (52).
A detailed description of the biochemical pathways underlying these events will be given in the following chapters.

### 1.1.2 Horizontal cells

A second type of neurons in the retina are the horizontal cells (HC). They span across cones and summate inputs from them to control the amount of GABA released back onto the photoreceptor cells, which hyperpolarizes them (105). Basically, when light is detected by a photoreceptor, the photoreceptor hyperpolarizes and reduces the release of glutamate. When this happens, HCs reduce the release of GABA, which leads to a depolarization of the photoreceptors (33). Their arrangement, together with the bipolar cells that receive input from the photoreceptors, constitutes a form of *lateral inhibition*, reducing redundancy in optic nerve signals and represents an important first step in scene analysis. Regions of spatially uniform illumination, which are highly redundant, evoke relatively little response, whereas regions containing contrast, which typically delineate the edges of objects in the enviroment, evoke strong responses (10).

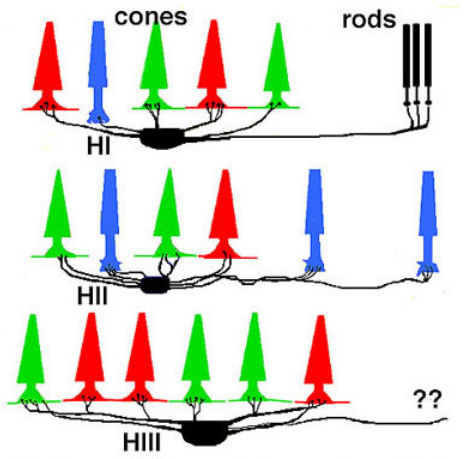


**Figure 1.5: Horizontal cell types in human retina** - *(from webvision.med.utah.edu)*

All mammalian retinas have at least two types of horizontal cells that function as the laterally interconnecting neurons in the outer plexiform layer (OPL), as shown in Figure 1.2. The cat retina organization has been studied extensively and the two types, known as A-type and B-type, have been well characterized (59). In the primate retina, instead, a third type has been identified (60). The HC types in the primate retina are known as HI, HII and HIII (see Figure 1.5).
**HI** is the classic horizontal cell of the primate retina. It is composed of a small dendritic tree (15-80 $\mu$m) that connects with cone pedicles and an axon that ends on rod spherule.
**HII** has a more intricate dendritic field than the other two types (61) and a short axon (100-200 $\mu$m). Both dendrites and axon are in connection with cone pedicles.
**HIII** cells are similar in appearence to HI cells, but bigger and asymmetrical in shape. The nature of the photoreceptor types that their axon contacts is still unclear.

### 1.1.3 Bipolar cells

Bipolar cells convey information from rods and cones to ganglion cells (see Figure 1.6). They receive synapses either from rods or cones and are classified as rod or cone bipolar cells respectively. There are roughly 10 distinct forms of cone bipolar cells and only one rod bipolar cell. Cone bipolar cells can be classified into two different groups, ON and OFF, based on how they react to glutamate released by photoreceptor cells. When light hits a photoreceptor, it hyperpolarizes, and releases less glutamate. An ON bipolar cell will react to this change, through a metabotropic glutamate receptor, by depolarizing its membrane. On the contrary, an OFF bipolar cell will react, through a ionotropic glutamate receptor, by hyperpolarization. On light stimulation, the photoreceptor reacts with a hyperpolarization, transmitter release ceases but the postsynaptic bipolar cells respond with either hyperpolarization or depolarization of their membranes (118).

### 1.1.4 Amacrine cells

While photoreceptors, horizontal and bipolar cells respond only with slow, graded changes in membrane potential, ganglion cells and some amacrine cells can generate spikes. Amacrine cells of the vertebrate retina are interneurons that interact at the second synaptic level of the vertically direct pathways consisting of the photoreceptor-bipolar-ganglion cell chain. They are synaptically active in the inner plexiform layer (IPL) (see Figure 1.2) and serve to integrate and modulate the visual message presented

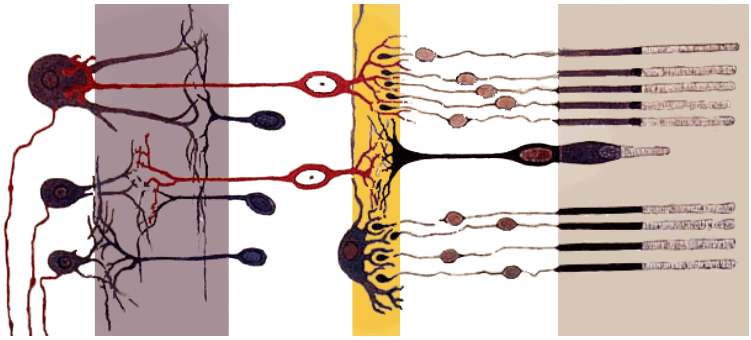

**Figure 1.6: Bipolar cells connect photoreceptors and ganglion cells** - Bipolar cells are indicated in red *(from Santiago Ramòn y Cajal, 1911)*

to the ganglion cell. Amacrine cells are so called because they are nerve cells initially thought to lack an axon as described by Cajal in 1892. Today we know that certain large field amacrine cells of the vertebrate retina can have long "axon-like" processes which probably function as true axons in the sense that they work as output fibers of the cell. Amacrine cells come in all shapes, sizes and stratification patterns and more subtypes are still being discovered with the Golgi staining method, intracellular recordings and immunocytochemical staining. Thus, at present, amacrine cells can be classified into about 40 different morphological subtypes. They are grouped on the basis of the width of their field of connection, the layer of the stratum in the IPL they are in, and the neurotransmitter type. Most of them are inhibitory using either GABA or glycine as neurotransmitters.

Relatively little is known about the functional roles of amacrine cells. Amacrine cells with extensive dendritic trees are thought to contribute to inhibitory surrounds by feedback at both the bipolar cell and ganglion cell levels, supplementing the action of the horizontal cells. Other types of amacrine cells are likely to be playing modulatory roles, allowing adjustment of sensitivity for photopic and scotopic vision. The AII amacrine cell (also known as the rod amacrine cell) is a mediator of signals from rod cells under scotopic conditions (58; 73; 77; 111; 113).

### 1.1.5 Ganglion cells

Ganglion cells are the final output neurons of the vertebrate retina. The ganglion cell collects the electrical messages concerning the visual signal from the two layers of

nerve cells preceding it in the retinal wiring scheme. A great deal of preprocessing is accomplished by the neurons of the vertical pathways (photoreceptor to bipolar to ganglion cell chain), and by the lateral pathways (photoreceptor to horizontal cell to bipolar to amacrine to ganglion cell chain) before presentation to the ganglion cell which represents the ultimate signalling component of retinal information to the brain. On average, ganglion cells are larger than most preceding retinal interneurons and have large diameter axons capable of passing the electrical signal, in the form of transient spike trains, to the retinal recipient areas of the brain many millimeters or centimeters distant from the retina. The optic nerve collects all the axons of the ganglion cells and this bundle of more than a million fibers then convey information to the next relay station in the brain for sorting and integrating into further brain processing pathways. There are about 1.2 to 1.5 million retinal ganglion cells in the human retina. With about 105 million photoreceptors per retina, on average each retinal ganglion cell receives inputs from about 100 rods and cones. However, these number vary greatly among individuals and as a function of retinal location. In the fovea (center of the retina), a single photoreceptor will communicate with as many as five ganglion cells. In the extreme periphery (ends of the retina), a single ganglion cell will receive information from many thousands of photoreceptors. Retinal ganglion cells spontaneously fire action potentials at a basal rate while at rest. Excitation of retinal ganglion cells results in an increased firing rate while inhibition results in a depressed firing rate (32; 53; 56; 77; 85; 129).
Based on their projections and functions, there are at least five main classes of retinal ganglion cells:

- **Midget ganglion cells** that project to the parvocellular layers of the lateral geniculate nucleus. They are characterized by slow conduction velocity and response to changes in color but they respond only weakly to changes in contrast. About 80% of retinal ganglion cells are midget cells.

- **Parasol ganglion cells** that project to the magnocellular layers of the lateral geniculate nucleus. They have fast conduction velocity, and can respond to low-contrast stimuli, but are not very sensitive to changes in color. About 10% of retinal ganglion cells are parasol cells.

- **Bistratified ganglion cells** that project to the koniocellular layers of the lateral geniculate nucleus. They are very small in size and have moderate spatial resolution, moderate conduction velocity, and can respond to moderate-contrast stimuli. About 10% of retinal ganglion cells are bistratified cells.

- **Other ganglion cells projecting to the superior colliculus** to control the pupillary light reflex and eye movements.

- **Photosensitive ganglion cells** that contain their own photopigment, melanopsin, which makes them respond directly to light even in the absence of rods and cones. They project to the suprachiasmatic nucleus (SCN) via the retinohypothalamic tract and are necessary to set and maintain circadian rhythms.

## 1.2 Phototransduction

Phototransduction is the process by which a photon of light generates an electrical response in a photoreceptor cell. This sophisticated and elegantly organized biochemical pathway has been intensely investigated for many decades and nowadays represents one of the best-characterized G-protein coupled signaling pathways. The first discovery in the field was done by Wilhelm Kuhne in 1879, who identified rhodopsin, the first G-protein coupled receptor (GPCR) (68; 69). The milestones in unraveling the phototransduction mechanisms were the discoveries of rhodopsin light-dependent phosphorylation (17; 67) and of the first arrestin protein and its relation with phosphorylated rhodospin (66; 126), the identification of the first cyclic nucleotide-gated channel (38) and in 2000, the rhodopsin crystal model, the first crystallographic structure of a GPCR (93).
The major steps of the phototransduction cascade (see Figure 1.7 for a schematic overview) are the following:

- **Rhodopsin photoisomerization:** the first step of the signalling cascade is the chromophore isomerization by a captured photon.

- **Transducin activation:** the activated rhodopsin interacts with the transducin complex, activating the $\alpha$-subunit by triggering the GDP-GTP exchange.

- **Phosphodiesterase activation:** the G$\alpha_t$-GTP stimulates the activity of the cGMP phosphodiesterase (PDE) by binding to its inhibitory subunit.
- **cGMP-channel closure**: Activation of the PDE results in a reduction of the intracellular level of cGMP thus causing the closure of the cGMP-gated channels (CNG channels). Closure of these channels results in the hyperpolarization of the photoreceptor.
- **Cascade inactivation:** Transducin activation ends when rhodopsin is multi-phosphorylated by rhodopsin kinase (RK). This event allows arrestin to bind to rhodopsin, which causes the final inactivation of the cascade.

This events will be extensively discussed in the following chapters.

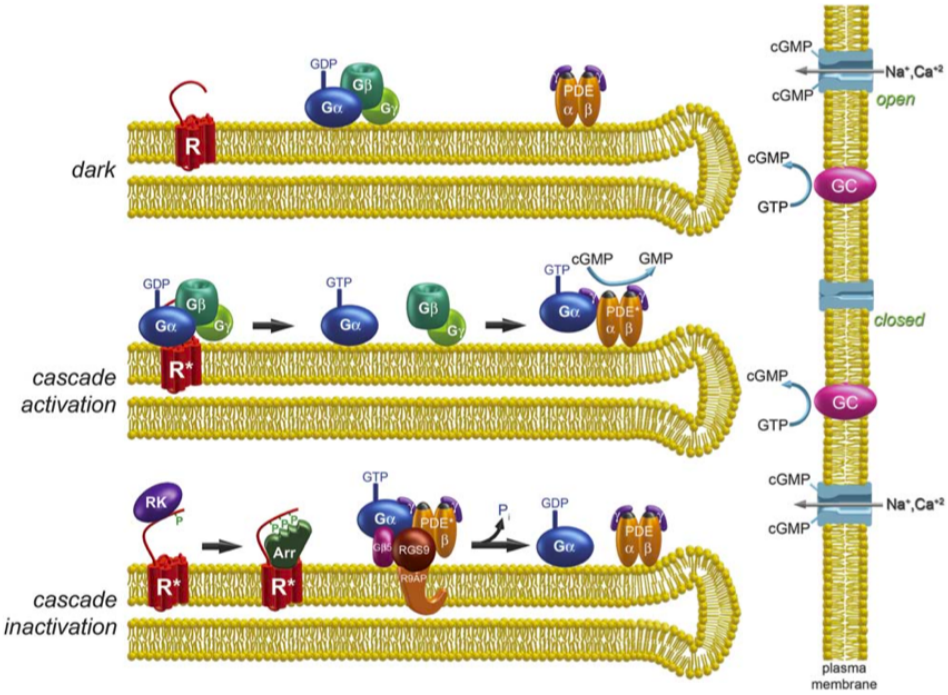


**Figure 1.7: Schematic of the phototransduction cascade** - The upper disc illlustrates inactive rhodopsin (R), transducin (G$\alpha$, G$\beta$ and G$\gamma$ subunits) and PDE ($\alpha$, $\beta$ and $\gamma$ subunits) in the dark. The reactions in the middle disc illustrate light-induced transducin and PDE activation. The reactions in the lower disc represent R$^*$ inactivation via phosphorylation by rhodopsin kinase (RK) followed by arrestin (Arr) binding and transducin/PDE inactivation by RGS9-G$\beta$5-R9AP complex. *(from Burns and Arshavsky, 2005 (20))*

### 1.2.1 Rhodopsin photoisomerization

Vision begins when a photon is captured by a chromophore molecule, inducing its chemical isomerization. The cromophore is a vitamin A derivative, the *retinal* that lies in a pocket formed by the seven transmembrane $\alpha$-helical domains of an opsin molecule. In humans, there are four different types of opsin involved in the visual process: one in the rods, three in the cones. Depending on their aminoacid sequences, the opsins tune the chromophore spectral sensitivity. Rhodopsin has its peak of sensitivity for light of 498 nm of wavelength.

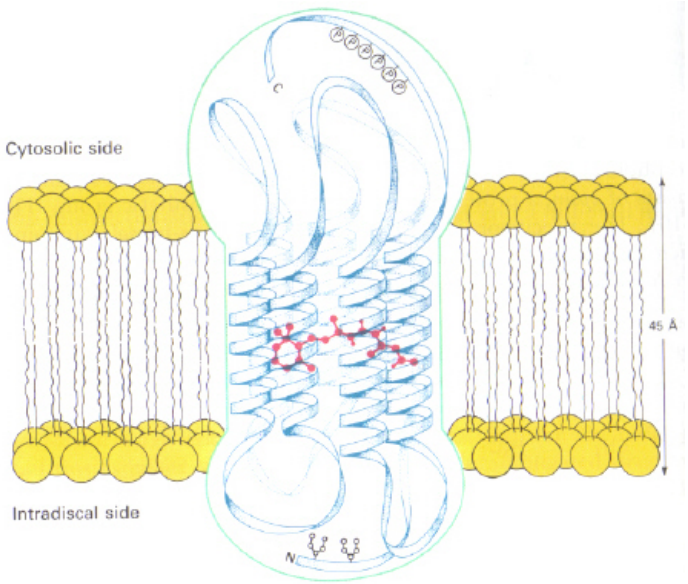


**Figure 1.8: The rhodopsin** - the figure shows the trans-membrane structure of the rhodopsin and the localization of the 11-cis-retinal *(from Stryer, L. "Biochemistry", $4^{th}$ edition, USA, Freeman and Company, 1999)*

In the quiescent state, the retinal molecule, in its 11-cis form, is bound to a lysine via a protonated Schiff-base bond. The capturing of a photon causes the photoisomerization of the retinal from its bent conformation to the straight all-trans form (as shown in Figure 1.9A). This event triggers some conformational changes that lead to the activation of the rhodopsin via four short-lived intermediates (see Figure 1.9B). The metarhodopsin II (or R*) is capable of activating the transducin, starting therefore the biochemical pathway. This is the first step of signal amplification, because a single

R* activates many transducin molecules in the course of its lifetime that ends once it binds arrestin. Subsequently, all-trans retinal detaches and diffuses away. The retinal molecules in all-trans form is recovered by the retinal pigment epithelium (RPE) cells in which they can be reconstitued in the 11-cis form. The resynthetized 11-cis retinal is transported to the photoreceptor, where it can bind an opsin, forming a new molecule of rhodopsin. This process is known as pigment regeneration.

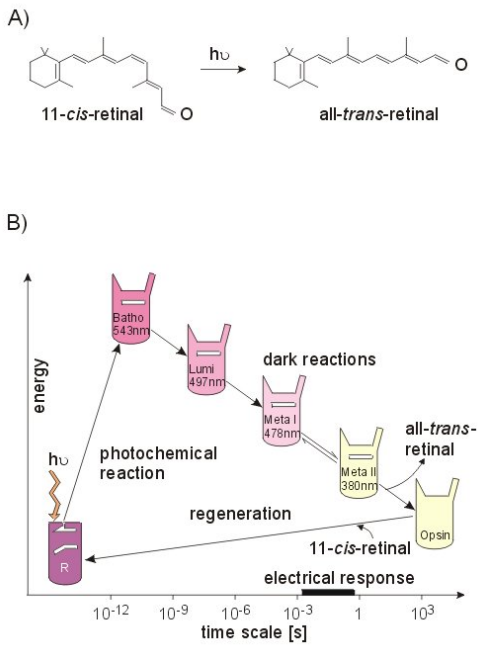


**Figure 1.9: Intermediate states of rhodopsin** - A: chemical isomerization of the retinal molecule; B: the five intermediate states during the activation of the rhodopsin *(from www.fz-juelich.de/ind/ind-1/Photoreception)*

### 1.2.2 Transducin activation

The second important step of the signaling cascade is the transducin activation by activated rhodopsin. Transducin belongs to the G protein family (guanine nucleotide-binding proteins), proteins involved in second messenger cascade. G proteins, discovered by Gilman and Rodbell (29; 76), function as "molecular switches", alternating between an inactive GDP- and an active GTP-bound state. G proteins are formed by two distinct families of proteins. Heterotrimeric G proteins, sometimes referred to as

the "large" G proteins, are activated by G protein-coupled receptors and made up of $\alpha$, $\beta$ and $\gamma$ subunits. There are also "small" G proteins (20-25kDa) that belong to the Ras superfamily of small GTPases. These proteins are homologous to the $\alpha$ subunit found in heterotrimers, and are in fact monomeric. However, they also bind GTP and GDP and are involved in signal transduction. Transducin belongs to the "large" G protein family and shares common features with its "relatives" such as activation in response to a conformation change in the G protein-coupled receptor, exchange of GTP for GDP and dissociation in order to activate further proteins in the signal transduction pathway (see Figure 1.10).

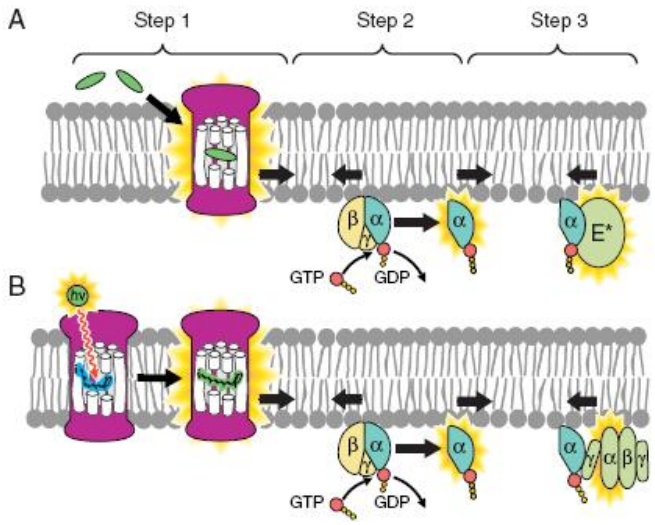


**Figure 1.10: Generic G protein signal cascade and in vertebrate phototransduction** - A. The cascade comprises three protein, a G protein-coupled receptor (R), a G protein (G), and an effector protein (E), which are activated in three steps. In the first step, the receptor R is activated to R*, and in most cases this is brought about by the binding of a ligand. In the second step, R* activates a specific G protein by catalyzing the release of GDP from the inactive form (G-GDP), and thereby permitting the binding of GTP, to create the active form G* (G-GTP) . A single R* can activate many molecules of G proteins, because it is released unaltered after the interaction. In the third step, the usual mechanism is that the G* binds to the effector protein E, causing it to switch state to an activate form E*. B. The G protein transduction cascade of vertebrate photoreceptors follows the general pattern shown in A, except that activation of R to R* is caused by the photoisomerization of a ligand, 11-cis retinal, that is already attached covalently to the receptor protein. *(from Pugh and Lamb, 2000 (101))*

In vertebrate phototransduction, the transducin complex is composed of one $\alpha$-subunit, one $\beta$-subunit and one $\gamma$-subunit and is anchored to the disc membrane. This adhesion is mediated by post-translational modifications of the subunits of the protein complex. Indeed, the $\alpha$-subunit is lauroylated and myristoylated on its N-terminal, while the $\gamma$-subunit is farnesylated on its C-terminal (40; 57). This anchoring limits the localization of transducin on the disc surface, facilitating the interaction between rhodopsin and its G protein.

Once activated by light, $R^*$ is able to interact with and bind to a transducin in its inactive form (G-GDP). This interaction leads to a conformational change in the $\alpha$-subunit structure, causing the dissociation of the GDP molecule. After loss of GDP, the transducin complex is free to encounter and bind a GTP molecule and this binding triggers a conformational change that leads to the dissociation of the activated G$\alpha$-GTP (also indicated as $G^*$) subunit from both $R^*$ and $\beta\gamma$ complex (see Figure 1.11). After dissociation, $R^*$ remains unaltered and is still able to activate hundreds of transducin molecules before its deactivation: this is a crucial step for the signal amplification through the signaling cascade (19; 51; 101).

Activated G$\alpha$-GTP binds to the inhibitory $\gamma$-subunit of the cGMP phosphodiesterase (PDE).

### 1.2.3 cGMP phosphodiesterase activation

The third element of the cascade is the cGMP-specific phosphodiesterase (PDE) that *de facto* is the "effector protein" (see Figures 1.10 and 1.11). PDE is composed of two catalytic subunits (PDE$\alpha$ and PDE$\beta$) and two identical inhibitory subunits (PDE$\gamma$). Since the rhodopsin is an integral membrane protein and transducin and PDE are anchored to the membrane, given that the C-terminals of the PDE $\alpha$- and $\beta$-subunits are isoprenylated and carboxymethylated (24; 25), all the interactions between these proteins are limited to the membrane surface.

The inhibitory PDE$\gamma$-subunit is the site of interaction with activated transducin. The G$\alpha$-GTP activates PDE by releasing the inhibitory activity of one of the PDE$\gamma$ subunits (131). It takes two G$\alpha$-GTP molecules to fully activate the holoenzyme. The activated PDE$\alpha$- and PDE$\beta$-subunits hydrolyze cGMP to 5'-GMP, causing a decrease in the cGMP intracytoplasmic concentration and leading to the closure of the cGMP-gated channel (19; 51; 101).

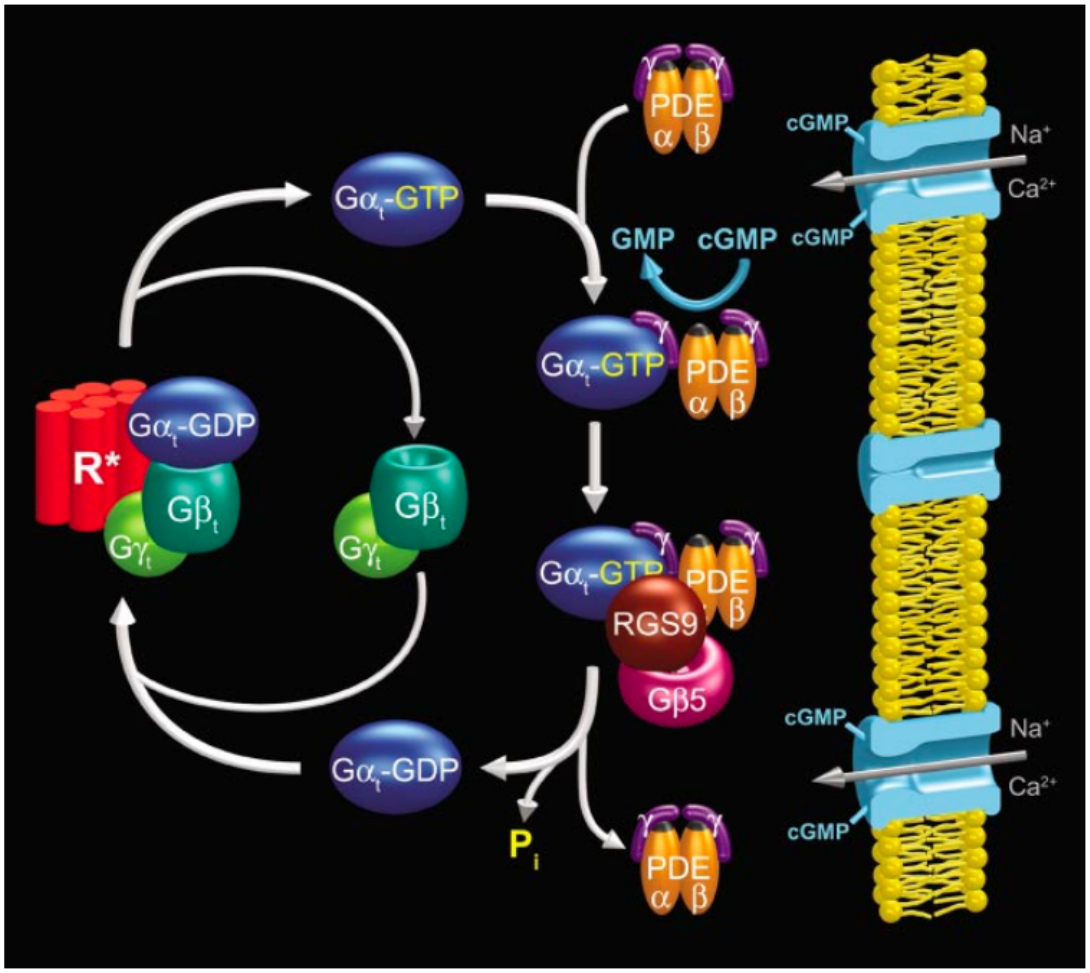


**Figure 1.11: The cycle of G protein activation and inactivation in phototransduction** - *(from Arshavsky et al., 2002 (3))*

### 1.2.4 cGMP-channel closure

The central molecule in phototransduction is the second messenger cGMP. All aspects of visual signaling are dictated by the balance between its synthesis and degradation in the cytoplasm of the photoreceptor outer segment: cGMP is synthetized by guanylate cyclase, whereas cGMP hydrolysis is performed by cGMP phosphodiesterase, activated by the process described above. In the dark-adapted photoreceptor, the balance between cGMP synthesis and hydrolysis produces a steady-state level of cGMP concentration. The free cGMP concentration is constantly monitored by cGMP-gated cation channels located in the outer segment plasma membrane. The inward current through these relatively non-specific cation channels keeps the cell partially depolarized. In the presence of light, cGMP levels decline as a result of PDE activation. The cGMP channels can sense the cGMP concentration and the low cytoplasmatic cGMP level prevents the channel opening. The channel closure causes the hyperpolarization of the cell and reduces the neurotransmitter release from the synaptic terminal, thus signaling the presence of light to the secondary neurons in the retina (20; 101).

### 1.2.5 Cascade inactivation

The shut-off of the phototransduction cascade requires the inactivation of the three activated intermediates, rhodopsin, transducin and phosphodiesterase.

#### 1.2.5.1 Rhodopsin inactivation

The lifetime of activated rhodopsin ($R^*$) determines the gain of the first step of the phototransduction cascade and the quencing of $R^*$ is the first necessary process in shutting off the cascade. $R^*$ shut-off is a two step mechanism that begins with the phosphorylation of the C-terminus of $R^*$ by rhodopsin kinase (RK) and ends with the binding of a 48 kDa accessory protein called arrestin (Figure 1.12).
The importance of the rhodopsin C-terminus for rhodopsin shut-off in vivo has been demonstrated. Transgenic mouse that express C-terminus truncated rhodopsin showed a prolonged and increased sensitivity to light responses, consistent with distrupted $R^*$ shut-off by RK phosphorylation (28). The crucial role of RK has been demonstrated by inactivating both alleles of the RK gene in a transgenic mouse. The elimination of the light-dependent phosphorylation of rhodopsin caused the single-photon response to

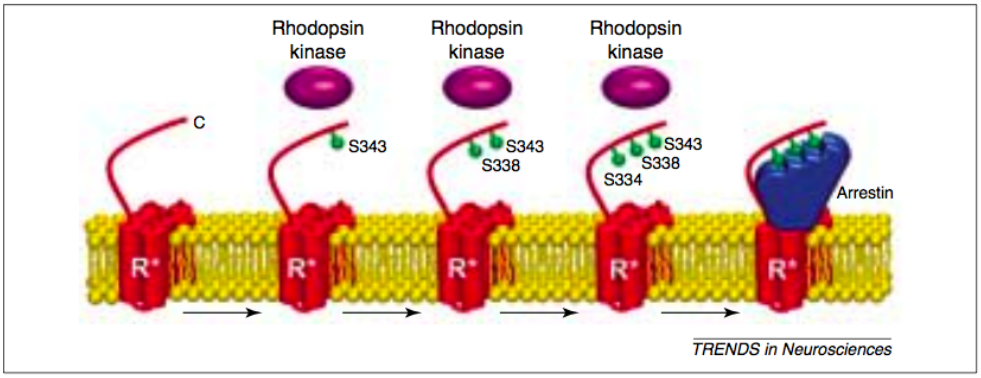


**Figure 1.12: Inactivation of photoexcited rhodopsin during the photoresponse by multiple phosphorylation and arrestin binding.** - *(from Arshavsky, 2002 (2))*

become larger and to last longer than normal (26). R* is phosphorylated on different sites ($Ser^{334}$, $Ser^{338}$ and $Ser^{343}$) and this modifications are critical for rhodopsin shut-off (78; 89; 125).

Rhodopsin phosphorylation by rhodopsin kinase is the first step in R* shut-off. Rhodopsin kinase belongs to a family of serine/threonine protein kinases, called G protein-coupled receptor kinases (GRKs) (91). Six GRKs have been identified so far and they are expressed in a wide variety of mammalian tissues. Rhodopsin kinase is a 63 kDa protein found exclusively in rods, cones and, in low levels, in the pineal gland. It is a cytosolic enzyme that translocates to the membrane upon receptor activation (55). The association of RK with the membrane is mediated by a post-translational modification in which an isoprenoid farnesyl is attached to the C-terminal cysteine residue (50).

RK is likely to be regulated by a 23 kDa calcium-binding protein called recoverin. The direct inhibition of rhodopsin kinase by recoverin is calcium-dependent (22; 27), suggesting that RK is inhibited in the dark when the intracellular calcium level is high and becomes disinhibited by the fall in calcium concentration during the light response.

The second step in R* inactivation is thought to be arrestin binding to phosphorylated rhodopsin (2; 125; 126). Arrestin binds to phosphorylated R* and prevents further activation of transducin by steric hindrance (65). In 1997, Xu *et al.* analyzed the photoresponse in rods from transgenic mice in which arrestin expression was either absent or reduced by half. Photoresponse recovery was found to be normal when expression was halved, indicating that arrestin binding is not rate-limiting for recovery

of the flash response. Photoresponse from rods completely lacking arrestin showed an initial partial recovery followed by a prolonged final phase, suggesting that there are both arrestin independent and dependent mechanisms involved in rhodopsin inactivation (128). Moreover, a frameshift mutation in the human arrestin gene causes Oguchi's disease, which is characterized by slowed dark adaptation (39).

Arrestin belongs to the family of the arrestins (37; 90), a large family of proteins found in both vertebrates and invertebrates, including distinct classes of visual arrestin, rod specific (45; 106; 107; 121), cone specific (1; 30; 31) and invertebrate specific (108; 130), and $\beta$-arrestins, which are involved in regulating responses to hormones (5). Visual arrestin (48 kDa) is expressed in photoreceptor cells and the pineal gland (14; 18). The expression pattern of visual arrestins is restricted to a few cell types, mainly in photoreceptors and pinealocytes (62). The onset of rod arrestin gene transcription in the mouse occurs before rod outer segment formation (16), whereas in the bovine retina, arrestin expression is concurrent with the espression of other genes involved in phototransduction (119). Arrestin protein is transcribed by the *Sag* gene (retinal S-antigen) (121).

There is also a 44 kDa splice variant of arrestin that binds to both phosphorylated and non-phosphorylated rhodopsin (109). The splice variant is truncated at the C-terminus and is membrane-associated suggesting that the C-terminal region of arrestin is responsible for its solubility (92; 102).

#### 1.2.5.2 Transducin inactivation

The second step in shutting off the phototransduction cascade is the turning off of the activated G$\alpha$-GTP (see Figure 1.7 and 1.13). Like the $\alpha$-subunit of all heterotrimeric G proteins, activated G$\alpha$-GTP has an intrinsic GTPase activity and turns itself off by hydrolyzing GTP to GDP. G$\alpha$-GDP is unable to stimulate PDE and reassociates with G$\beta\gamma$ ending the G$\beta\gamma$ lifetime as well. Although G$\alpha$-GTP is able to hydrolyze bound GTP by itself, the intrinsic rate of this GTPase activity is very slow compared to the time course of photoresponse. This slow GTPase rate is significantly accelerated by a multi-protein complex with GAP-like (GTPase activacting protein) properties, containing member 9 of the regulators of G protein signaling protein family (RGS9)(44), bound to its obligatory G$\beta$5 subunit (75) and membrane anchor R9AP (49). Patients with mutations in RGS9 or R9AP show slow photoreceptor deactivation and have

difficulty in adjusting to changes in light levels, as well as in seeing low-contrast, moving objects (88).

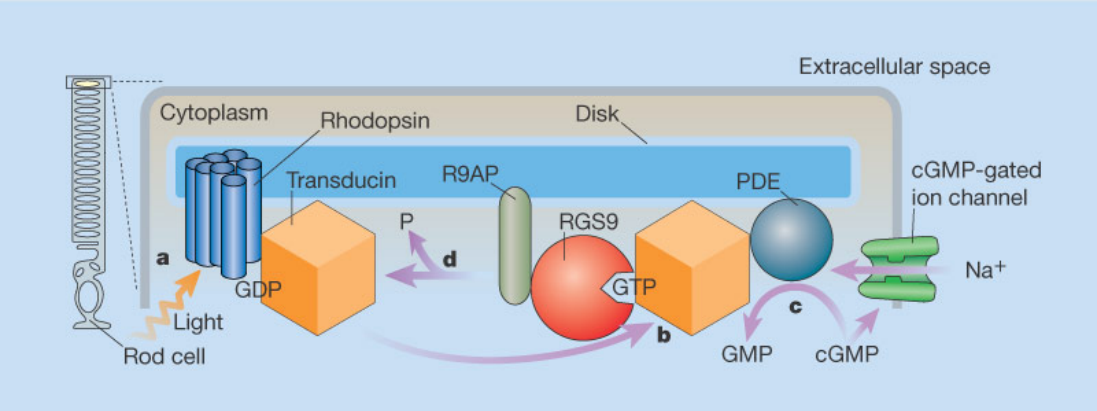


**Figure 1.13: Activation and Inactivation of transducin** - In the rod class of photoreceptors, the pigment-containing protein rhodopsin absorbs light (a) and activates transducin (b) by causing it to release GDP and bind GTP. GTP-bound transducin binds to and activates a phosphodiesterase (PDE), which converts cGMP to GMP (c). The concentration of cGMP decreases below what is required to open cGMP-gated ion channels, reducing the flow of ions across the cellular membrane. RGS9 bound to R9AP turns off the light-induced response by accelerating the rate of GTP hydrolysis by transducin, releasing phosphate, P (d). Other proteins that regulate the phototransduction cascade have been omitted for clarity. *(from Blumer, 2004 (15))*

#### 1.2.5.3 Phosphodiesterase inactivation and cGMP resynthesis

The final step in photoresponse shut-off is quenching of activated PDE. The reassociation of the inhibitory PDE$\gamma$ subunit with PDE$\alpha$ and $\beta$ catalytic subunits, when G$\alpha$ hydrolizes GTP to GDP, prevents further cGMP hydrolysis. The PDE$\gamma$ binding has been localized in the catalytic sites of PDE$\alpha$ and $\beta$ subunits (4).

Complete recovery of the photoresponse requires not only inactivation of cascade components, but also the restoration of cytoplasmic cGMP to the dark level. This is accomplished by two isoforms of guanylate cyclase, GC1 (or GC-E) and GC2 (or GC-F) (6; 99). However, the decrease in cGMP concentration caused by PDEis not sufficient to induce sufficiently rapid resynthesis of cGMP by the cyclase. The enzymatic rate of cyclases is increased indirectly through changes in intracellular $Ca^{2+}$ concentration.

Light causes a decline in the outer segment $Ca^{2+}$ because $Ca^{2+}$ continues to be extruded from the cell via the $Ca^{2+}K^{+}/Na^{+}$ exchanger, while its entry through the CNG channels is reduced (46; 83). The fall in intracellular $Ca^{2+}$ is sensed by $Ca^{2+}$ binding proteins called guanylate cyclase activating proteins (GCAPs), which rapidly stimulate cGMP synthesis by guanylate cyclase (34; 95; 96).

GCAPs are $Ca^{2+}$-binding proteins, belonging to the calmodulin gene superfamily but in contrast to calmodulin, which is active in the $Ca^{2+}$-bound form, GCAPs stimulate GCs in the $Ca^{2+}$-free form and inhibit GCs upon $Ca^{2+}$ binding. The human and mouse GCAP1 and GCAP2 genes (*Guca1a* and *Guca1b*) are organized in a tail-to-tail array (genes arranged on opposite strands) separated by relatively short intergenic regions containing polyadenylation sites for transcript termination (47; 117).

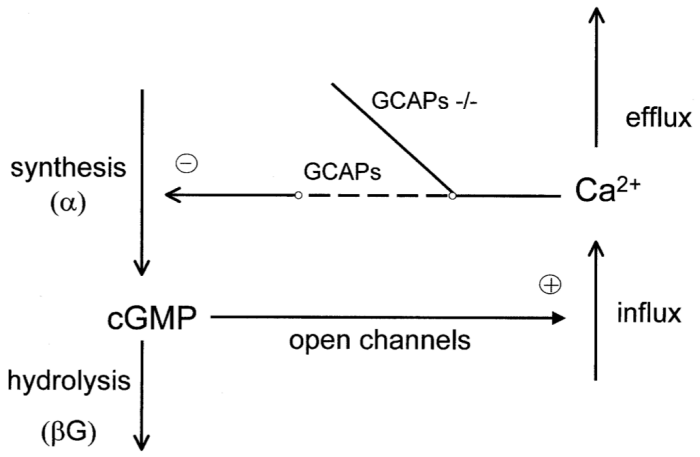


**Figure 1.14: The negative feedback loop that regulates cGMP concentration in rod cells** - A change in the cGMP concentration changes the number of open channels and the size of the inward current, part of which consists of $Ca^{2+}$ influx. The alteration in $Ca^{2+}$ influx changes the internal $Ca^{2+}$, which in turn changes the rate of cGMP synthesis in the direction that opposes the initial change. Deletion of GCAPs expression opens the feedback loop ($GCAPs^{-}/^{-}$). *(from Burns et al., 2002 (21))*

The $Ca^{2+}$/GCAP-dependent regulation of guanylate cyclase activity forms a powerful feedback mechanism (see Figure 1.14) in which the rate of cGMP synthesis increases as $Ca^{2+}$ concentration drops during photoresponse. The abolishment of $Ca^{2+}$ feedback by knocking out GCAPs results in photoresponses that are much larger than normal and somewhat prolonged (79). In addition, loss of GCAPs leads to a dramatic increase

in the fluctuations in cGMP concentration in the dark (21), which arises primarly from spontaneous rhodopsin and PDE activation (11). Consequently, $Ca^{2+}$ feedback to the cyclase activity sets the photoresponse amplitude, enhances temporal response properties and improves the signal-to-noise characteristics of the rod.

## 1.3 Light adaptation mechanisms

Light adaptation refers to the ability of photoreceptors to adapt their sensitivity as the level of ambient illumination changes; the range of light intensities could span over more than ten orders of magnitude. Light adaptation causes mainly two effects on the photoresponse. It decreases the response amplitude to incremental changes in illumination and speeds response kinetics. In doing so, it rescues the cell from saturation that would otherwise occur at relatively low light intesities. Light adaptation is mediated by many mechanisms, some of them will be discussed in this chapter.

### 1.3.1 Calcium-dependent adaptation

$Ca^{2+}$ plays the lead role in light adaptation, several mechanism are dependent by intracellular level of $Ca^{2+}$. Bownds first proposed that steady light might produce a decrease in intracellular level of $Ca^{2+}$ (13) and subsequently a role for $Ca^{2+}$ in light adaptation was indicated by the experiments of Torre et al. on salamander photoreceptors (120). Nowadays, it is well-known how $Ca^{2+}$ acts and three $Ca^{2+}$-dependent mechanisms have been characterized: (a) regulation of guanylate cyclase activity, (b) regulation of rhodopsin kinase activity via recoverin and (c) regulation of the CNG channel sensitivity to cGMP.

The first mechanism occurs via GCAPs. As described above, the activity of these proteins are $Ca^{2+}$-regulated, therefore the fall of intracellular $Ca^{2+}$ activates the GCAP-regulation of the guanylate cyclase consequently speeding the rate of cGMP synthesis. In doing so, the cytoplasimc level of cGMP is maintained despite the high light-activated PDE activity (96).

A second $Ca^{2+}$-dependent mechanism consists in the regulation of rhodopsin kinase (RK) activity by recoverin. Recoverin is a $Ca^{2+}$ binding protein and interacts with RK in $Ca^{2+}$ bound state, inhibiting its ability to phosphorylate rhodopsin (27; 54). Light-dependent reduction in intracellular $Ca^{2+}$ relieves this inhibition and leads to a more

rapid R* inactivation and ultimately to a lower level of PDE activity (63). Experiments on recoverin knockout mice indicate that this regulation has its major effect on bright light responses and responses in steady light (74).

The third mechanism mediated by $Ca^{2+}$ is the modulation of the sensitivity of the CNG channels by calmodulin (9; 48). In the dark, $Ca^{2+}$ bound calmodulin is associated with an intracytoplasmic domain of the channel. The light-dependent $Ca^{2+}$ fall causes the calmodulin dissociation to increase the channel's sensitivity to cGMP. This allows channels to report small changes in cGMP when cGMP concentration becomes very low. However, the overall effect of this sensitivity modulation in rods is thought to be relatively small.

### 1.3.2 Other forms of adaptation

The light-dependent increase in steady-state PDE activity underlies a $Ca^{2+}$-indipendent and very powerful mechanism that adjusts photoreceptor sensitivity and it is simply a direct consequence of phototransduction. In the dark, when the PDE activity is low, few photons produce a large change in the cGMP concentration and therefore a measurable electrical response. On the contrary, in the light, the same amount of photons produces a smaller relative increase in PDE activity and a smaller cGMP decrease. Experiments conducted on rod salamander showed that the rate constant of cGMP hydrolysis increases ∼20 times from dark to light-adapted value (86; 87).

Most studies addressing the mechanisms of light adaptation have been performed under conditions where light of relatively low intensity has been applied for relatively short times. In 2002, Calvert *et al.* described two distinct temporal phases in bullfrog rods. The fast phase, that operates within seconds after the onset of illumination, is consistent with the well characterized $Ca^{2+}$-dependent feedback mechanisms and can desensitize the rods as much as 80-fold. The slow phase occurs instead after tens of seconds of continuous illumination and only at light intensities that suppressed more than half of the dark current. This second mechanism provides an additional sensitivity loss of up to 40-fold before the rod saturates. Thus, rods can achieve a total degree of adaptation of ∼3000-fold. Nevertheless, the molecular mechanism underlying the slow phase is still unclear (23).

#### 1.3.2.1 Light-induced protein translocation

Another possible mechanism contributing to light adaptation may be the light-driven redistribution of some protein components of the cGMP cascade of the visual transduction between the outer and the inner segment (see Figure 1.15).

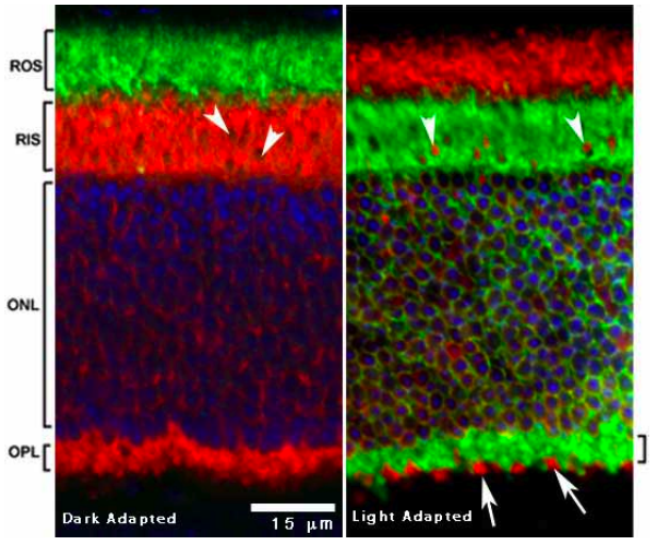


**Figure 1.15: Light-dependent translocation of arrestin and rod $\alpha$-transducin** - Immunocytochemical localizations of arrestin and rod $\alpha$-transducin in dark and light adapted albino mouse retinas were conducted. In the dark, arrestin (red) is localized in the RIS, ONL, and OPL whereas $\alpha$-transducin (green) is localized in the ROS. The localizations are reversed in the light adapted retinas with the arrestin localized to the ROS and $\alpha$-transducin being in the RIS, ONL, and OPL. Cone inner segments show up as red streaks (arrow heads) in the region of the RIS in the light adapted retina and the cone terminals appear as red spots (arrows) in the OPL. Nuclei are stained with DAPI. The rod outer segment is indicated by ROS, the rod inner segment is indicated by RIS, the outer nuclear layer is indicated by ONL, and the outer plexiform layer is indicated by OPL. The scale bar represents 15 $\mu$m. *(from Elias et al., 2004 (35))*

First evidence of this was given by Philp *et al.* in 1987; their studies showed as the immunocytochemical localization of transducin and arrestin (but not PDE phosphodiesterase) changed according to light conditions. In particular, transducin was concentrated in the outer segments of photoreceptor cells in dark conditions while in the light transducin was seen in the inner segments and in the outer nuclear layer. On the contrary, arrestin had the opposite distribution, appearing in the inner segment and outer

nuclear layer in dark conditions and in the ROS under light conditions (98). These movements appear to be initiated directly by the absortion of light by rhodopsin (124). The hypothesis of an adaptive role for the light-dependent translocation of transducin and arrestin was proposed by Sokolov *et al.* that also quantified the rate of transducin translocation by serial tangential sectioning of light- or dark-exposed retinas (110). Subsequent studies were conducted to characterize the nature of the biological mechanism. Experiments conducted in ATP-depleted photoreceptors indicate that the distribution of arrestin in rods is controlled by its dynamic interactions with rhodopsin in the OS and microtubules in the IS and its movement is an energy-indipendent process and occurs by simple diffusion (82). The translocation temporal kinetics for the two proteins were found to be slightly different. In fact, transducin translocates in less than two minutes from the onset of light whereas the translocation of the majority of arrestin requires at least five to six minutes. Translocation in the opposite direction, from light to dark, occurs more slowly for both proteins with arrestin requiring almost 30 minutes and transducin needing more than 200 minutes to complete its journey (35).

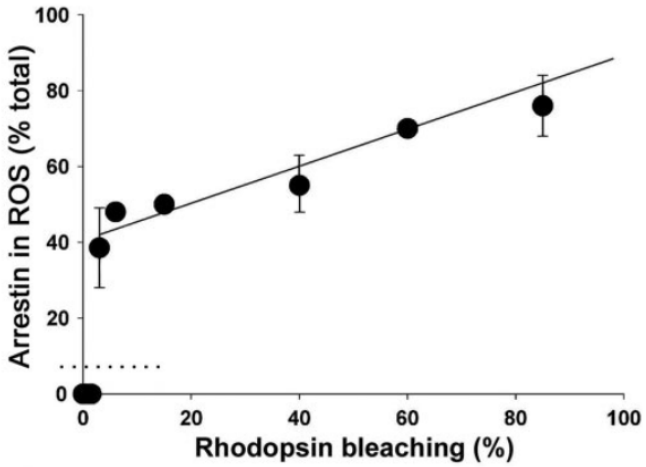


**Figure 1.16: Light-dependency threshold of arrestin translocation** - Arrestin distribution in the rods of anesthetized mice kept in the dark or after 30 min of steady illumination at various intensities was analyzed by serial sectioning/Western blotting. Continuous light producing up to ∼580 R*/rod/s (bleaching up to 1.5% rhodopsin during the entire illumination period) did not cause any detectable arrestin translocation. However, just by doubling the light intensity to produce ∼1160 R*/rod/s (bleaching 3% rhodopsin during the experiment) triggered the translocation of ∼36% of the total arrestin pool. *(from Strissel et al., 2006 (115))*

Successively, it was found that arrestin translocation is triggered when the light intensity approaches a critical threshold corresponding to the upper limits of the normal range of rod responsiveness, and that the amount of arrestin entering the rod outer segments under these conditions is superstoichiometric to the amount of photoactivated rhodopsin, as shown in Figure 1.16 (115).
The possible translocation of other proteins was also studied: recoverin was found to undergo light-dependent localization in the same directions of transducin while no translocation of rhodopsin kinase or GCAPs was identified (114).
Even if Sokolov *et al.* reported that the transducin translocation from outer segment correlates with a reduction in cascade amplification with a nearly 10-fold effect occurring in saturating light (110), the contribution of arrestin and recoverin translocation in light adaptation still has to be determined.

# 2

# Materials & methods

## 2.1 Microarray on isolated photoreceptors

### 2.1.1 Harvesting of isolated photoreceptors from mouse retinas

Dark-adapted C57/Bl6 mice were sacrificed under an infrared light source and photoreceptors were isolated enzymatically and mechanically using a buffer containing papain 0.1%, DNAse 400U, NaCl 150 mM, KCl 3.5 mM, $CaCl_2$ 1 mM, $MgCl_2$ 2.4 mM, HEPES 5 mM, D-Glucose 10 mM, incubating for 3 min at 37°C. After dissociation, samples were plated in two different dishes and positioned on two distinct set-ups: one always in the dark under infrared light and the other under 10 lux light. Small aggregates of isolated photoreceptors were harvested every 5 min with suction pipettes. The harvested cell aggregates were expelled into 50 $\mu$l of Trizol (Invitrogen) on ice and stored at -80°C.

### 2.1.2 Global polyadenylation PCR amplification (GA)

Total RNA from each sample was isolated from Trizol (Invitrogen) following the addition of 100 ng of polyinositol. RNA recovery by precipitation in isopropanol was optimized by using linear polyacrylamide (Ambion) as a carrier. All of the harvested RNA was resuspended in 4.5 $\mu$l of ice-cold cell reverse transcription mixture containing: 47 $\mu$l lysis buffer (100 $\mu$l 10x PCR buffer (Roche), 60 $\mu$l 25 mM $MgCl_2$ (Roche), 5 $\mu$l of NP-40 (American Bioanalytical), 50 $\mu$l of 0.1 DTT (Gibco/Invitrogen), 725 $\mu$l of DEPC-treated water), 1 $\mu$l RNAse inhibitors mix (1:1 prime RNA inhibitor (Eppendorf) and RNAguard$^{TM}$ Ribonuclease Inhibitor (Porcine)), 1 $\mu$l anchor T primer

(final concentration 200ng/ml), 1 $\mu$l 2.5 mM dNTP (LA Takara). Total RNA was reverse transcribed to cDNA, tailed with poly-A and amplified for 30 cycles of PCR as described by Subkhankulova and Livesey (116). PCR products were purified with the CyScribe GFX Purification kit (Amersham Biosciences) and directly labelled for microarray hybridization with dCTP-Cy3/Cy5 (Amersham) with the BioPrime DNA labelling system (Invitrogen).

### 2.1.3 Microarray hybridization and data analysis

Expression microarrays containing 23232 65-mer oligonucleotides (Sigma-Genosys) were printed on Codelink slides (Amersham). Hybridized arrays were scanned in an Axon microarray scanner at a resolution of 10 $\mu$m at maximum laser power and photomultiplier tube voltage of 60-80%. Image and feature analysis were performed with GenePix Pro 4.0 (Axon Instruments, Inc.). Statistical analysis of microarray data was conducted in the R environment using the R package "Statistics for Microarray Analysis". Data normalization was performed using scaled loess normalization (Limma package) (123). Differentially expressed genes were selected and clustered using Maanova package, according to their temporal expression pattern (http://www.jax.org/staff/churchill/labsite/).

## 2.2 Real-time PCR

### 2.2.1 Animals

All mouse and rat experiments were carried out according to the Italian and European guidelines for animal care (d.l.116/92; 86/609/C.E.). C57/Bl6 mice and Long Evans rats were bred and maintained under a 12 hour light/dark cycle (7AM:7PM). For lighting environment changes, two groups of overnight dark-adapted animals were maintained in either a darkened or a lighted cage. A 60W bulb was used as an adjustable light source. For each time point at least six animals were sacrificed by cervical dislocation, the eyes enucleated, the lenses removed and the retinas collected in Trizol (Invitrogen).

### 2.2.2 Cultured retinas

The retina culture system was established according to the experimental procedures previously published by Reidel and colleagues in 2006 (103). In brief, intact eyes of

postnatal day 21 C57/Bl6 mice were immediately removed from sacrificed animals and incubated with 1.2 mg/ml Proteinase K (Sigma-Aldrich) for 15 min at 37°C. Proteinase K activity was stopped by transferring the eyes to the culture medium containing 10% fetal calf serum for 5 min. After rinsing the eyes four times in serum-free culture medium for Proteinase K removal, retinas were dissected in basal culture medium after removal of the sclera, ocular tissue and the hyaloid vessel under preservation of the pigmented epithelium as described in Figure 2.1. Retinas were spread with the retinal pigmented epithelial cells facing down on ME 25/31 culture membranes (Schleicher and Schuell, Germany), cultured in Dulbeccos Modified Eagles Medium with F12 supplement (DMEM-F12) and 10% fetal calf serum, penicillin and streptomycin (Sigma-Aldrich) and maintained at 37°C with 5% $CO_2$. They were cultured for 2 days in 12L:12D cycle ($\lambda$=520 nm) before light/dark experiments. After light or dark exposure, cultivated retinas were collected in Trizol (Invitrogen).
For the acute rat retina experiments, retinas were isolated under dim red light from adult Long Evans rats and prepared for culturing as described for the mouse organotypic culture. Retinas were dark adapted for two hours and than exposed to the same light intensities used during ERG experiments equivalent to 410 and 2000 Rh*/r/s.

### 2.2.3 Real-time PCR protocol

Total RNA from retinas was extracted according to the manufacturers instructions (Invitrogen). In brief, retinas were homogenized in 1 ml of Trizol by passing several times through a glass pipette. After adding 0.2 ml of chloroform, samples were centrifuged at 14000 rpm at 4°C for 20 min. After centrifugation, RNA containing acqueus phase was collected in a fresh tube. Subsequently, RNA was precipitated by adding 0.5 ml of isopropyl alcohol overnight at -20°C. RNA was then pelleted by centrifuging at 14000 rpm at 4°C and washed with 70% ethanol in DEPC-treated water (14000 rpm at 4°C for 20 min). RNA pellets were resuspended in 10 $\mu$l RNAse-free water (Qiagen). RNA was further purified using an RNeasy column (Qiagen) and quantified using an ND-1000 Nanodrop spectrophotometer (Nanodrop Technologies). Total RNA (500 ng) was treated with DNAse I (Invitrogen) to remove any genomic DNA contamination and converted to cDNA using Superscript II reverse transcriptase (Invitrogen).
Twenty microliter PCR reaction mixtures contained cDNA, SYBR green master mix (Bio-Rad), $H_2O$ and custom primers designed for each gene of interest. The PCR

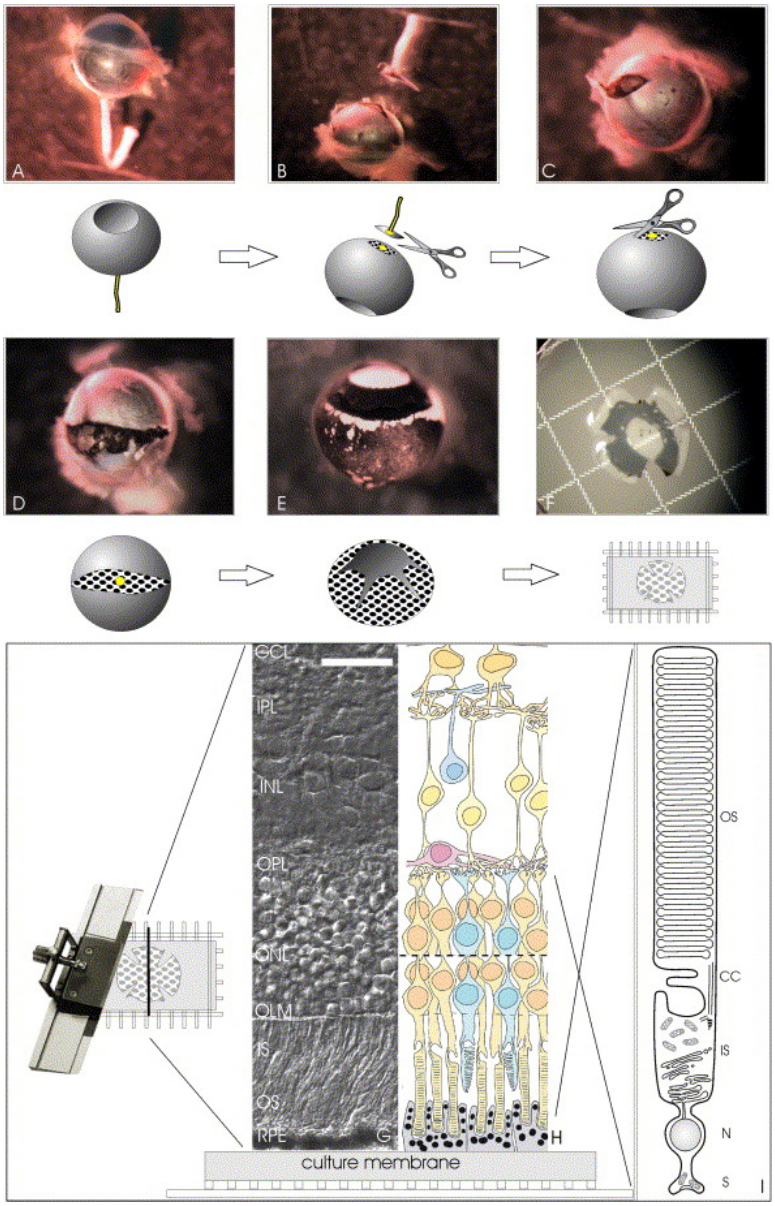


**Figure 2.1: Dissection and preparation of organotypic retina culture** - A: Eyeball with optic nerve prepared from a sacrificed mouse. B: Cutting off the optic nerve under slight tension with forceps. C: Incision of sclera by gently inserting scissors between the retinal pigmented epithelium and the sclera. D: Complete incision of sclera around eyeball to each side reaching the cornea. E: Incisions in the retinal cup, previously removed from sclera, cornea, lens, vitreous, iris, and hyaloid vessel. F: Flattening of spread retina on culture membrane attached to nylon spacer. G: Differential interference contrast picture of a retinal cryosection indicating the orientation of retinal explant with pigmented epithelium attached to the culture membrane. H: Schematic representation of retina and cell organization. I: Schematic representation of vertebrate photoreceptor cell. Scale bar, 13.2 $\mu$m *(from Reidel et al., 2006)*(103).

reactions were performed in an iQ5 thermocycler (Bio-Rad). Each reaction was performed at least in duplicate, and threshold cycles (CT) were calculated using the second derivative of the reaction. The CT of each gene was normalized against that of the control reference transcript Gapdh. Fold changes were determined using the -ΔΔCT method, using the average of dark control set to zero (71; 97; 133). RNA controls were performed to ensure that amplification of products did not come from genomic DNA contamination.

Primers used for Real-Time PCR:

| | |
|---|---|
| Gapdh mouse for: | GCTGCCCAGAACATCATCCC |
| Gapdh mouse rew: | ATGCCTGCTTCACCACCTTC |
| Sag mouse for: | TTACAAGCCTTCCAACCTCTGAC |
| Sag mouse rew: | ACCAGCACAACACCATCTACAG |
| Pde6b mouse for: | TGCTGACTGTGAGGAGGATGAG |
| Pde6b mouse rew: | GGGAATCTGGAACTTTCGGACTAC |
| Guca1a mouse for: | CCCTCAGCCAGCCAGTATGTG |
| Guca1a mouse rew: | ACTTCTGTTCCACTTTGCCCTTG |
| Gapdh rat for: | CAAGTTCAACGGCACAGTCAAGG |
| Gapdh rat rew: | ACATACTCAGCACCAGCATCACC |
| Sag rat for: | GTGTCATACCATATCAAAGTGAAGC |
| Sag rat rew: | GGAACGGCACCTCAGTAGC |
| Guca1a rat for: | CAACGGGGATGGGGAACTG |
| Guca1a rat rew: | GGTCAAGTCCAGGCTTCGG |
| Guca1b rat for: | GCTTCTTCAAGGTCACTGGTAATG |
| Guca1b rat rew: | GTAGATTGCCTCCACGATGTCC |
| Sag intron rat for: | CCCTTGCCCTGTGAGGTTATCTG |
| Sag intron rat rew: | ACCTTGTAATTTGTCACCGAAGTCAG |
| Guca1a intron rat for: | CCCTCAGCCAGCCAGTATGTG |
| Guca1a intron rat rew: | CTTCCCATCCCTCCCGTCCTC |
| Guca1b intron rat for: | TTCTTCAAGGTCACTGGTAATG |
| Guca1b intron rat rew: | GATGGAAAGGTCACTCAATGG |

## 2.3 Immunohistochemistry

### 2.3.1 Arrestin translocation detection

Enucleated eyes were prefixed in PFA 4% in PBS for 30 minutes. Successively, eyecups obtained after lens and sclera removals were fixed in PFA 4% overnight. The lens removal allows fixative to penetrate the tissue diffusely. After fixation, samples were cryoprotected with scalar dilution of sucrose (10%, 20% and 30%), embedded in O.C.T. (Sakura Tissue-Tek OCT Compound) and cryosectioned at 16 $\mu$m at -20°C.

Immunolabeling was performed by standard protocols using anti-arrestin PA1-731 (Affinity BioReagents, Golden, CO) as primary antibody and DAPI (Boehringer Mannheim GmbH, Germany) for nuclear staining.

### 2.3.2 TUNEL assay

Terminal Transferase dUTP Nick End Labeling (TUNEL) Assay is a method used to detect DNA degradation in apoptotic cells because one of the hallmarks of late stage apoptosis is the fragmentation of nuclear chromatin which results in a multitude of 3-hydroxyl termini of DNA ends. This property can be used to identify apoptotic cells by labeling the DNA breaks with fluorescent-tagged deoxyuridine triphosphate nucleotides (F-dUTP).

Retinal cryosections, processed as described in the previous section, were rinsed in PBS 1× and permeabilized with 0.1% Triton X-100 and 0.1% Sodium Citrate for 2 minutes at 4°C. Subsequently, 100 $\mu$l of TUNEL reaction mixture (Chemicon) were added to each slide and kept for 60 minutes at 37°C in a humid chamber. After washing in PBS, 100 $\mu$l of 1:1000 DAPI (Boehringer Mannheim GmbH, Germany) were applied for 5 minutes at room temperature for nuclear staining. Slides were mounted with Vectashield (Vector Laboratories Inc., Burlingame, CA) for microscopy analysis. The positive control was treated, after permeabilization, with DNase I solution (100 $\mu$l of 200 $\mu$g/ml) for 10 minutes at room temperature. In the negative control reaction mixture, terminal transferase enzyme was omitted.

## 2.4 Western blotting

Retinas, dissected from light or dark-exposed mice, were homogenized in Lysis buffer (50 mM Tris pH 7.5; 150 mM NaCl; 1% Triton X-100; 10 mM $MgCl_2$) in ice. The total amount of protein was determined using BCA protein assay kit (Pierce Biotechnology). The homogenate was diluted with sample buffer, subjected to scalar dilutions, run on SDS-PAGE and Western blotted using the following antibodies: rabbit anti-visual arrestin (PA1-731, Affinity Bioreagents, Golden, CO), mouse anti-GCAP1 (MA1-724, Affinity BioReagents, Golden, CO), rat anti-HSC70 (SPA-815, StressGen) and rabbit anti-$\beta$-tubulin III (Sigma-Aldrich, Italy). HSC70, heat-shock cognate protein 70, and $\beta$-tubulin III are constitutively expressed proteins and were used as control of protein loading. Signals were detected analyzing the optical density of the spots.

## 2.5 Electroretinogram

### 2.5.1 Animal preparation for ERG recording

All animals were dark-adapted overnight. Anaesthesia was induced by intraperitoneal injection of urethane 120mg/100g (Sigma-Aldrich) (12; 41; 80). This was sufficient to maintain the animal deeply anesthetized throughout the entire experimental session, as verified by the absence of corneal reflexes. The general conditions were continuously monitored by recording the electrocardiogram (ECG). Body temperature was maintained at 37°C with an electric blanket. Pupils were dilated with 1% tropicamide (Sigma-Aldrich). A thin layer of methylcellulose solution (Lacrinorm, Farmigea) protected the cornea.

### 2.5.2 Optical stimulation

Full field illumination of the eyes was obtained via a Ganzfeld sphere (30 cm diameter), the interior surface of which was coated with a highly reflective white paint. An electronic flash unit (SUNPAK B3600 DX) generated a stimulus and its energy decayed in time ($\tau$=1.7 ms). Saturating a-wave responses were obtained by delivering flashes of white light, the scotopic efficacy of which was evaluated according to Lyubarsky and Pugh (72). The estimated retinal illuminance was $1.4 \times 10^5$ $Rh^*$/rod/flash. A steady background was obtained by illuminating the Ganzfeld sphere with 4 green

light emitting diodes (LEDs) with a $\lambda = 520$ nm (Opto Diode Corp.). Fluctuations of the background light intensity were less than 13% during the entire lenght of the experiments.

### 2.5.3 ERG recording

ERGs were recorded in a completely darkened room via coiled gold electrodes making electrical contact with the moist cornea. A small gold plate placed in the mouth was used as reference. Responses were amplified differentially, band-pass filtered at 0.3-500 Hz, digitized at 0.078 ms intervals by a PC interface (National instruments LabVIEW 6.1, Italy). Responses to flashes were averaged with an interstimulus interval of 60 s and measured at fixed intervals after background exposure up to 240 minutes. Since a typical experimental session spanned over a relative long period of time (4 to 5 hours), special care was paid to perform recordings at the same time of the day (starting at midday), in order to minimize the influence of circadian rhythms on ERG measurements (7; 8; 112).

### 2.5.4 Measurements of the pupil size

The pupil size was estimated by measuring its radius at the beginning and at the end of the ERG recording session. A digital camera was used in the red eye removal mode and the pupil radius measured by an image analysis software (GIMP 2.4.2). In control experiments, we measured the diameter of the pupil (as shown in Figure 2.2A). In these experiments, changes of pupil area were within 25% of their initial value, measured at the beginning of the experiment. Collected data from 7 experiments show that the pupil diameter is not significantly changed from start to end of the experimental session lasting at least 4 hours (as shown in Figure 2.2B).

## 2.6 Light estimation

### 2.6.1 Light intensities and equations

In the freely moving animal experiments, the light intensities were measured using an Illuminometer (mod. 5200, Kyoritsu Electrical Instruments Works, LTD). Since the animals were free to move and their pupils were not dilated by any pharmacological

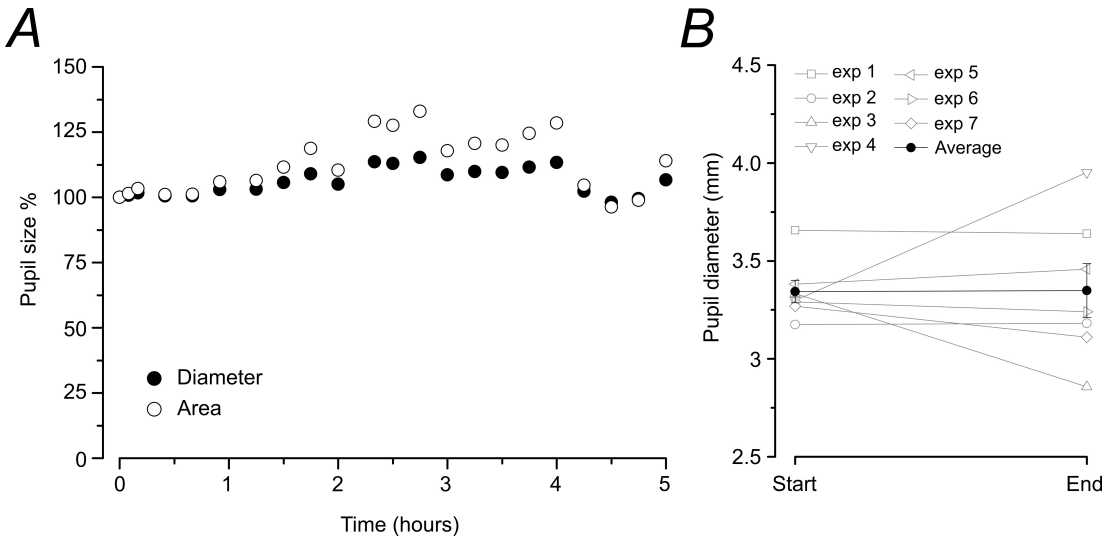


**Figure 2.2: Change of pupils diameter and area during long ERG sessions** - A: time course of pupil diameter (filled circle) and area (open circle) for a representative experiment. Pupil was dilated with 1% tropicamide. B: changes of pupils diameter in 7 experiments from start to end (4-5 hours later) of the ERG recording sessions. Averaged pupil diameter (filled circles) in mm±SEM: initial: 3.34±0.06; final: 3.35±0.14 (n=7; paired t-test: $p = 0.97$, not significant).

treatment, only an estimation of the cage illumination in lux (stated as ambient light) was given.

For ERG and organotypic cultures experiments, the light intensities were measured using a Radiometric probe (Model 818-ST, Newport corp., Irvine, CA) connected to a Optical Power Meter (Model 1815-C, Newport corp., Irvine, CA).

The number of photoisomerizations in a single rod per second $\Phi/\Delta t$ was estimated using the equations 2.1, 2.2 and 2.3.

$$F(\lambda) = \frac{I}{E_{photon}} = \frac{I}{h\frac{c}{\lambda}} \tag{2.1}$$

where: $F(\lambda)$ is the photon density [photons $m^{-2}$ $sec^{-1}$], $I$ is the measured irradiance [W $m^{-2}$], $h$ is the Planck constant ($6.626 \times 10^{-34}$ J $sec^{-1}$), $c$ is the speed of light in a vacuum ($2.99792 \times 10^{8}$ m $sec^{-1}$) and $\lambda$ is the light wavelength [m];

$$\frac{\Phi}{\Delta t} = F(\lambda) \cdot \tau(\lambda) \cdot a_c(\lambda) \frac{S_{pupil}}{S_{retina}} \tag{2.2}$$

where: $\Phi/\Delta t$ is the estimated Photoisomerization per rod per second, $\tau(\lambda)$ is the transmission of the pre-photoreceptor ocular media (estimated as 1 in cultures and 0.7 in ERG), $a_c(\lambda)$ is the "end-on collecting area" of the photoreceptor [$m^2$] (0.20 $\mu m^2$ in P21 mouse cultures and 1.3 $\mu m^2$ in ERG and in rat acute retinas) and $S_{pupil}$, $S_{retina}$ are the areas of the pupil and the retina, respectively [$m^2$] ($S_{pupil}/S_{retina} = 1$ in culture and 7.1/55 in ERG);

$$a_c(\lambda) = f\frac{\pi d^2}{4}[1 - 10^{-\Delta D(\lambda)L}]\gamma \tag{2.3}$$

where: $f$ is the funneling factor (1.3), $d$ is the outer segment diameter (estimated 1 $\mu$m for the P21 photoreceptor), $\Delta D(\lambda)$ is the specific axial density of rhodopsin (0.019 o.d. units $\mu m^2$), $L$ is the lenght of outer segment (estimated 8 $\mu$m for the P21 photoreceptor) and $\gamma$ is the quantum efficiency of photoisomerization (2/3).

### 2.6.2 Bleaching levels

In white mice and rats, pigment regeneration has been reported to occur with a time constant of around 30 min, about 4× slower than in humans (70). It is known that many general anesthetics can cause even further lowering of the regeneration rate but there are no evidences in literature about the effect of urethane on pigment regeneration.

**Table 2.1:** Estimation of the bleaching levels in ERG experiments

| Light Intensity ($Rh^*/r/s$) | % of bleaching after 4h ($\tau_{fast} = 30min$) | % of bleaching after 4h ($\tau_{slow} = 120min$) |
|---|---|---|
| 2000 | 3.60% | 12.45% |
| 410 | 0.73% | 2.55% |
| 60 | 0.11% | 0.37% |

We have estimated the level of bleaching for our ERG experiments, when the pigment regeneration is considerably slowed by anesthesia ($\tau_{slow} = 120$ min) and in the case in which it is fast ($\tau_{fast} = 30$ min) (see table 2.1).

# 3

# Results

In my studies, I addressed the issue of whether illumination could influence the rate of transcription of genes involved in phototransduction and how these changes could be involved in physiological processes.
Therefore, changes in gene expression were investigated in different light/dark conditions in several preparations: small aggregates of isolated photoreceptors, in cultivated intact retinas and in retinas acutely isolated from freely moving mice and rats. However, rods dissociated from mice and rats retinas are extremely fragile and usually degenerate after 2 hours of intense light exposure. Retinas extracted from intact animals are in better physiological conditions, but the extracted mRNAs derives from all retinal neurons, although the rodent retina is composed of approximately 70% rod photoreceptors (81).

## 3.1 Microarray analysis in isolated photoreceptors

Photoreceptors from dark-adapted retinas were isolated under infrared light, subjected to presence or absence of light and harvested at different time points. Single rod photoreceptors isolated from rodent retinas are fragile and often show clear signs of loss of morphological integrity after 2 hours of light exposure. Therefore, harvesting was restricted to small groups of photoreceptors and not to isolated rods and was not performed after 120 minutes. Moreover, they are easy to identify because of rods peculiar shape and for this reason contamination from other cell types can be easily avoided. Small aggregates of isolated photoreceptors were positioned on the perfusion chamber

of two distinct set-ups: one set-up was kept in complete darkness and mechanical manipulations were performed in infrared light; the other set-up was kept in a constant light of 10 lux (see Figure 3.1 for a schematical representation of the experimental protocol).

Rod photoreceptors were harvested from both set-ups in a time interval of up to 2 hours and grouped in three categories: those exposed to a short period of light (harvesting time from 0 to 40 minutes, n=14 bunches of rods), those exposed to an intermediate period of light (from 40 to 80 minutes, n=22) and those exposed to a long period of light (from 80 minutes up to 2 hours, n=16). The mRNA extracted from isolated photoreceptors predominantly came from rods.

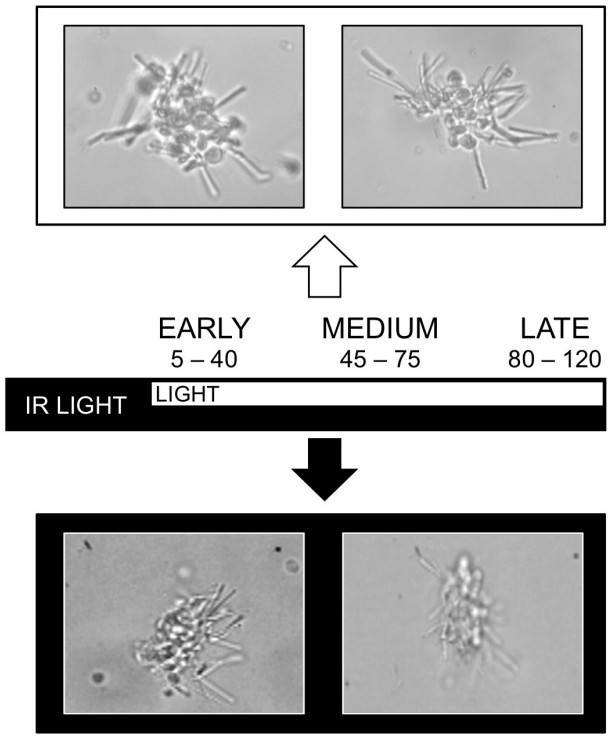


**Figure 3.1: Microarray analysis in isolated photoreceptors: scheme of harvesting procedure** - Dark-adapted retinas were dissociated under infrared illumination. Small bunches of rods were harvested simultaneously every 5 minutes in both dark and light conditions. Rods were grouped into three different categories for early (from 0 to 40 minutes; n=14), medium (from 40 to 80 minutes; n=22) and late (from 80 minutes up to 2 hours; n=16) changes of gene expression. The light intensity impinging on the set-up used for harvesting light adapted rods was approximately 10 Lux.

After harvesting, mRNA obtained from groups of rods was amplified by global polyadenylation PCR amplification technique (GA). This technique is the approach of choice to obtain the largest possible number of the differentially expressed genes, starting from a very low amount of RNA (116) . The scheme of amplification is represented in Fig. 3.2.

The gene expression was profiled using custom-made two-channel oligonucleotide arrays representing over 22000 genes. Each light-exposed sample was amplified and hybridized with a proper reference sample (dark) and each hybridization was repeated twice, inverting the Cy3/Cy5 dyes. The results were obtained analyzing 26 sample gene profiles from 52 microarray slides.

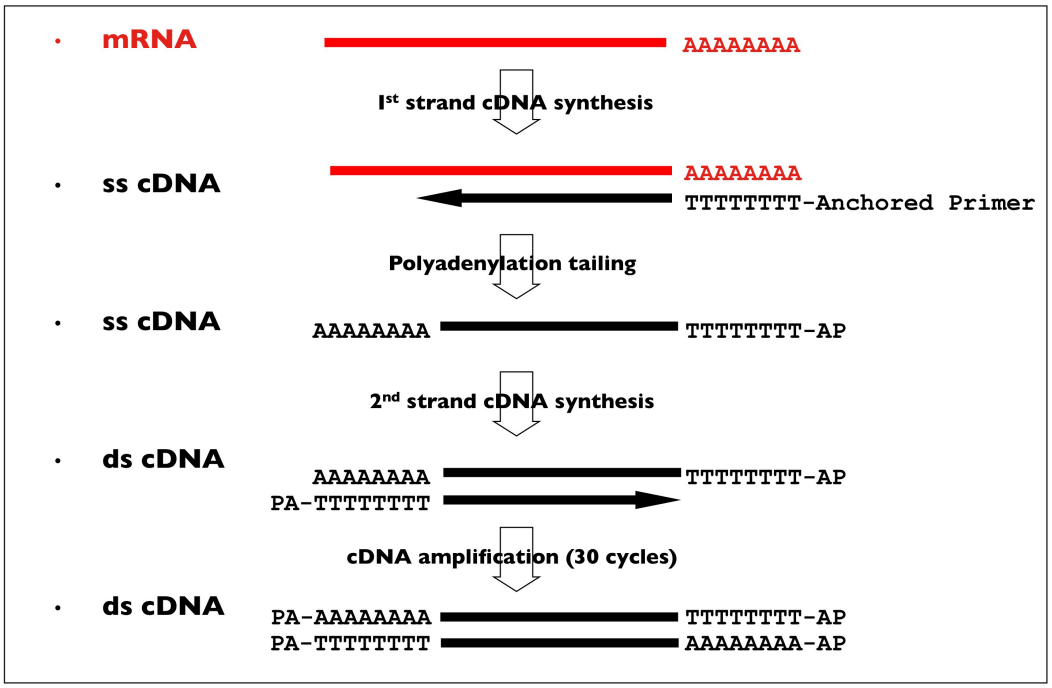


**Figure 3.2: Global polyadenylation PCR amplification (GA)** - Each RNA sample was retrotranscribed and subsequently amplified following the scheme

1933 genes exhibited significant changes of gene expression and were grouped in 10 different clusters, according to their temporal expression pattern (Maanova Package) (Figure 3.3). One cluster (termed cluster 10) had 74 genes up-regulated by more than two-fold, specifically for the long light exposure period and contained several genes

coding for proteins involved in phototransduction (Figure 3.4).

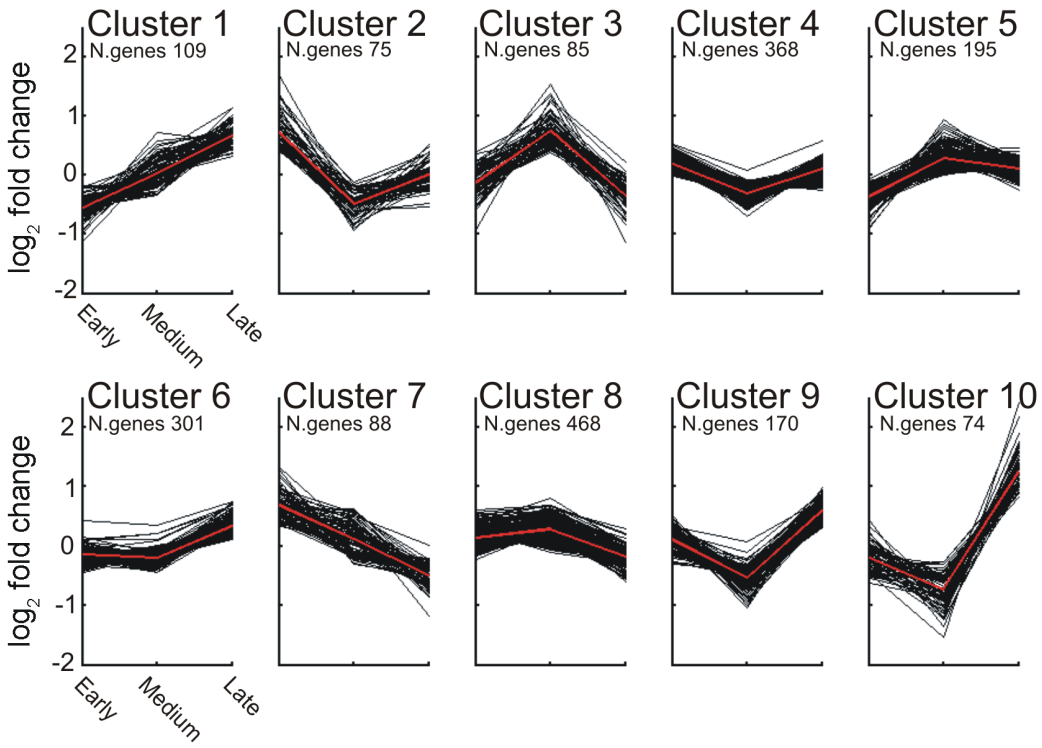


**Figure 3.3: Microarray analysis in isolated photoreceptors: clustering** - Time course of changes in gene expression in the ten cluster after a short, intermediate and long light exposure; cluster centroid indicated in red.

In this cluster, 7 genes known to be part of the phototransduction machinery were found: arrestin (*Sag*), the beta subunit of phoshodiesterase (*Pde6b*), the guanylate cyclase activator 1a (*Guca1a*), the guanine nucleotide binding protein, alpha transducing 1 (*Gnat1*), opsin-1 cone pigment (*Op1sw*), Unc-119 homolog C. elegans (*Unc119*) and the rod outer segment membrane protein 1 (*Rom1*). This cluster also contained 7 genes coding for crystallins (*gamma S, gamma B, beta A4, beta B2, alpha A, gamma D* and *beta A1*). As shown in Figure 3.4, this cluster contained also genes coding for protein transport (5), protein modification (4), protein translation (4), mRNA processing (4), apoptosis (3) and other functions (15). The remaining 25 genes had an unknown function.

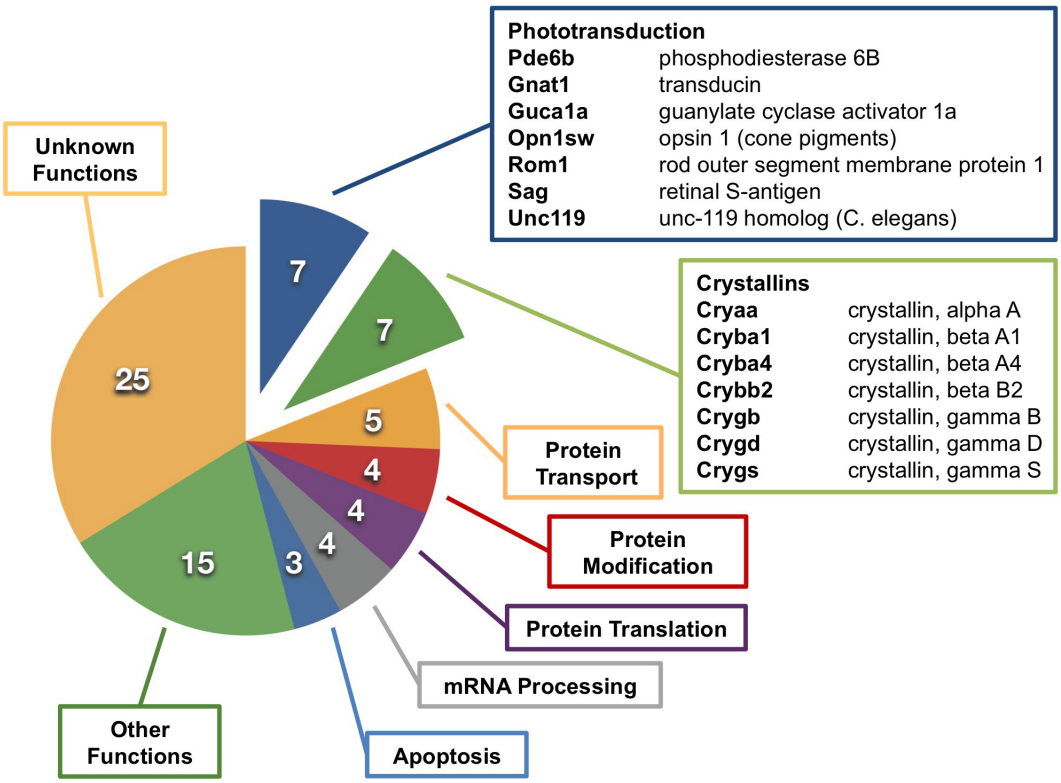


**Figure 3.4: Microarray analysis in isolated photoreceptors: gene ontology** - Gene Ontology analysis of genes in Cluster 10.

## 3.2 Real-time PCR analysis for selected genes in retinas from intact mice

Three of the up-regulated genes reported in Figure 3.4 are particularly relevant for phototransduction: *Sag*, *Guca1a* and *Pde6b*. Indeed up-regulation of genes activating guanylate cyclase, such as *Guca1a* and *Guca1b*, would be expected to elevate the cGMP level, while up-regulation of *Sag* would be expected to reduce the ability of photo-isomerized rhodopsin to close cGMP gated channel. As a consequence, up-regulation of *Guca1a*, *Guca1b* and *Sag* is likely to reactivate the photocurrent and thus to contribute to light adaptation.

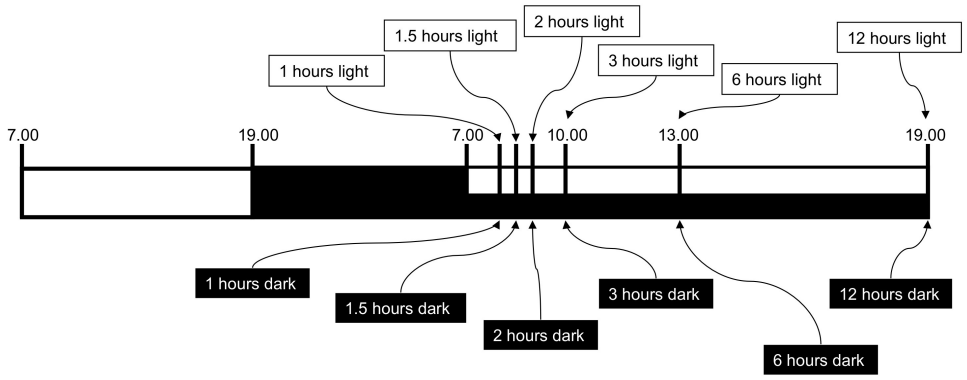


**Figure 3.5: Scheme of protocol for the Real time PCR analysis experiment in freely moving mice** - For each time point, two cohorts of mice, normally held in 12 hours light/12 hours dark cycle, were taken in different light conditions. After sacrifice, time course of changes in expression induced by light was performed in harvested retinas.

Therefore, the changes in expression of *Sag*, *Guca1a*, *Guca1b*, *Pde6b* and *Gnat1* were analyzed with real-time PCR in retinas extracted from freely moving mice kept in complete darkness and mice exposed to a continuous light (see Fig. 3.5). Since these genes are known to be expressed exclusively or primarily in rod photoreceptors, changes in their expression detected in whole retinas are due to changes occurring in rod photoreceptors (42; 96). Under these conditions, long light exposures can be used without photoreceptor deterioration (see below in Fig. 3.12), unlike in dissociated rod photoreceptors.

Changes in gene expression at each time point were obtained using at least 6 pairs of retinas from mice kept in 1000 lux ambient light (test condition) and 6 pairs of retinas from mice kept in darkness (control condition). The ratio in $\log_2$ units of observed changes are shown in Figure 3.6. After 2 hours of light exposure, the level of mRNA for *Sag*, *Guca1a* and *Guca1b* increased approximately by 1.75-fold from the dark level. *Sag*, *Guca1a* and *Guca1b* transcripts remained elevated at longer times, up to 6-12 hours. Changes in *Pde6b* transcript levels were statistically significant ($p<0.05$), but were smaller in magnitude, whereas the changes in *Gnat1* expression were not statistically significant ($p>0.1$).

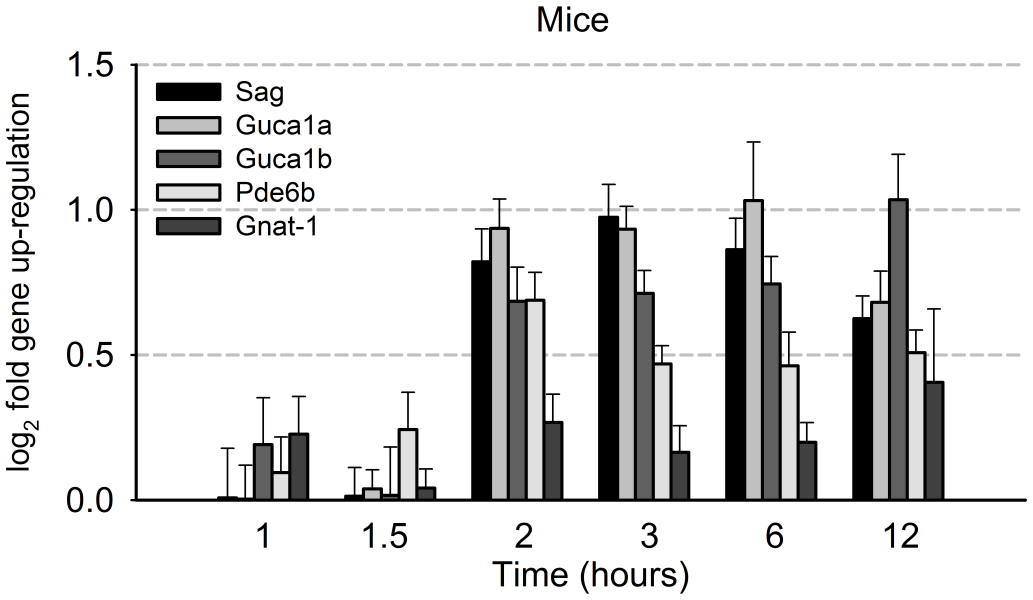


**Figure 3.6: Real time PCR analysis in retinas from freely moving mice** - Time course of changes in expression (relative to the control level in dark conditions) induced by light of *Sag*, *Guca1a*, *Guca1b*, *Pde6b* and *Gnat1* genes in retinas harvested from freely moving mice exposed to an ambient light of 1000 lux. Light exposures varied from 1 to 12 hours. Each point is the average obtained from at least 6 pairs of retinas (mean±SEM).

Having established that light elevated the rate of transcription of genes coding for *Sag*, *Guca1a* and *Guca1b* we asked whether the elevated mRNA levels were maintained upon returning to darkness and, if so, for how long. In order to do this, we exposed mice to a steady light for 2 hours followed by complete darkness for 2 hours. After this treatment, transcripts for *Sag*, *Guca1a* and *Guca1b* were still elevated but to a lesser

extent (Figure 3.7A). These results indicate that the light-dependent up-regulation of *Sag*, *Guca1a* and *Guca1b* persisted transiently returning to darkness, decaying with a time constant of approximately 2 hours.

We also analyzed the dependence of up-regulation of *Sag*, *Guca1a* and *Guca1b* expression on light intensity. As shown in Figure 3.7B, 2 hours exposure to an ambient light between 250 lux and 500 lux produced an half maximal gene up-regulation for the three studied genes.

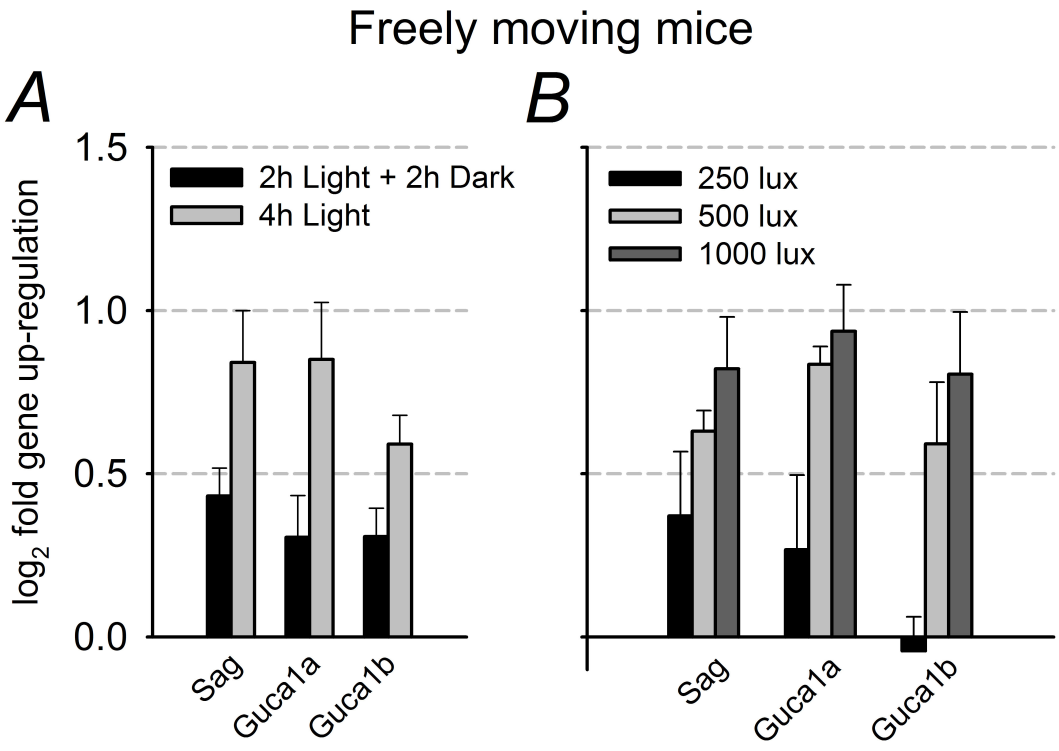


**Figure 3.7: Real time PCR analysis in retinas from freely moving mice and in cultured retinas** - (A) Changes in gene expression observed in retinas extracted from freely moving mice exposed to 1000 lux ambient light for 2 hours followed by 2 hours of darkness compared to retinas from mice kept for 4 hours in the same light. As a control, a group of mice were kept for 4 hours in the dark. Each point is the average of at least 3 experiments (mean±SEM). (B) Relation between changes in gene expression and ambient light intensity in freely moving mice exposed at 250, 500 and 1000 lux after 2 hours of illumination. Each point is the average from at least 6 pairs of retinas (mean±SEM).

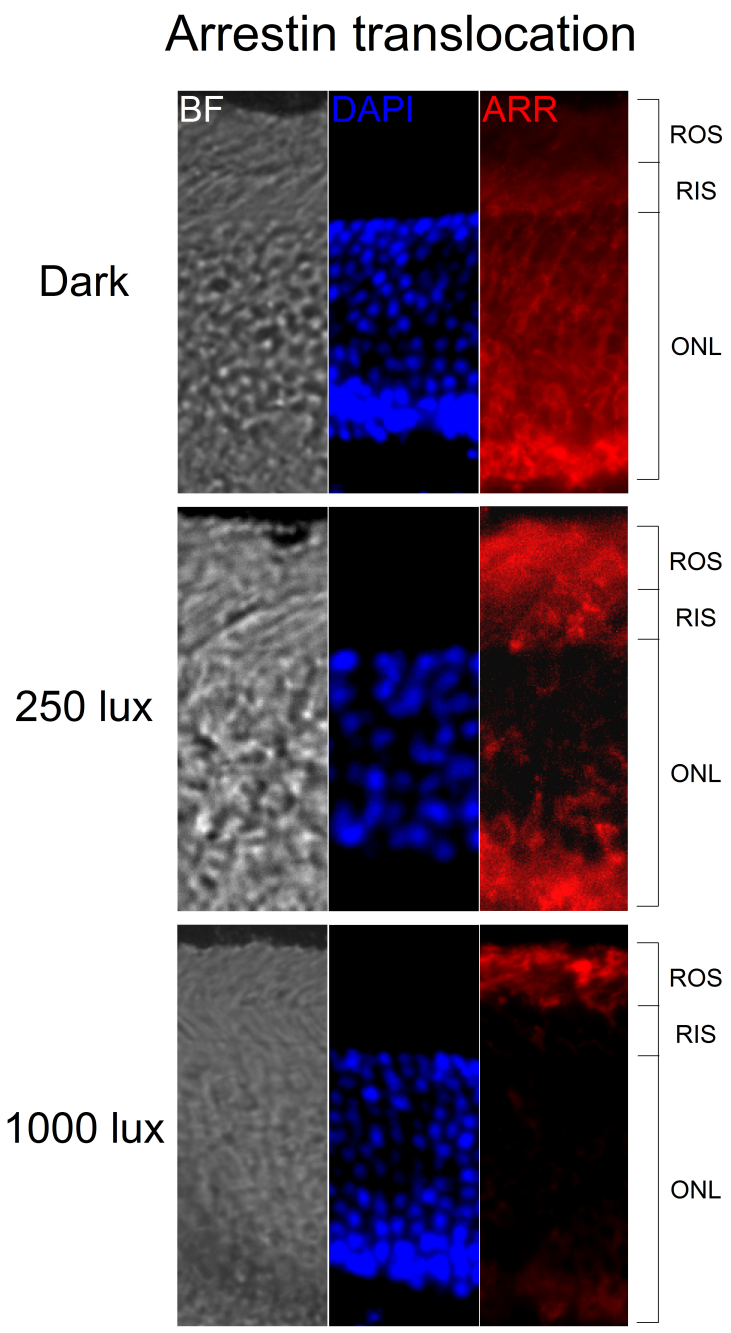


**Figure 3.8: Arrestin translocation in retinas from freely moving mice** - IF images of light-dependent arrestin translocation, following 2 hours of illumination in retinas extracted from freely moving mice. Arrestin migration occurs from the outer nuclear layer (ONL) and rod inner segments (RIS) (in the dark), to rod outer segments (ROS) when mice are kept in a bright ambient light of 1000 lux. A partial migration is observed when the ambient light was decreased to 250 lux. Columns from left to right show bright field images (BF), nuclear localization with DAPI staining in blue and arrestin labeling in red (ARR).

As arrestin is known to migrate from the cell body and inner segment towards the outer segment upon light exposure, we correlated the level of up-regulation of expression with arrestin migration towards rods outer segments. Freely moving mice were exposed to different ambient lights for 2 hours and control animals were kept in the dark. After dissection, half of these retinas were used to quantify gene expression by real-time PCR and the remaining retinas were used to determine arrestin migration by immunofluorescence staining. As shown in immunofluorescence images (Figure 3.8), arrestin migrates completely towards the outer segment in the brightest light conditions for which maximal gene up-regulation was observed. At a lower light (250 Lux), a partial migration of arrestin towards the outer segments was observed and transcripts coding for *Sag*, *Guca1a* and *Guca1b* were up-regulated to a sub-maximal level (n=6). Therefore, light-dependent gene up-regulation and arrestin translocation (115) occured in the same range of light intensity.

## 3.3 Western blot analysis for proteins coded by selected genes

In order to verify whether up-regulation of *Sag*, *Guca1a* and *Guca1b* genes resulted in an increased level of related protein, the expression level of arrestin and GCAP1 was determined by quantitative Western blotting (Figure 3.9) from retinas of freely moving mice. We were not able to quantify expression level of GCAP2 due to lack of a reliable commercial antibody against that specific mouse protein.

For the quantitative Western blot analysis, different lines with scaled concentrations of retinal homogenates were selected, in order to carry out analyses in dark adapted conditions and in retinas exposed to a steady bright light equivalent to 1000 Lux for 3 hours. Western blot analysis showed that the concentration of both forms of arrestin, the full-length with a molecular weight of 48kDa and its splice variant with a molecular weight of 44kDa (92; 102), increased by approximately 57% (Figure 3.9C) and GCAP1 by 36% (Figure 3.9D) after 3 hours of light exposure. This proved, as expected, that gene up-regulation leads to an increase in protein synthesis.

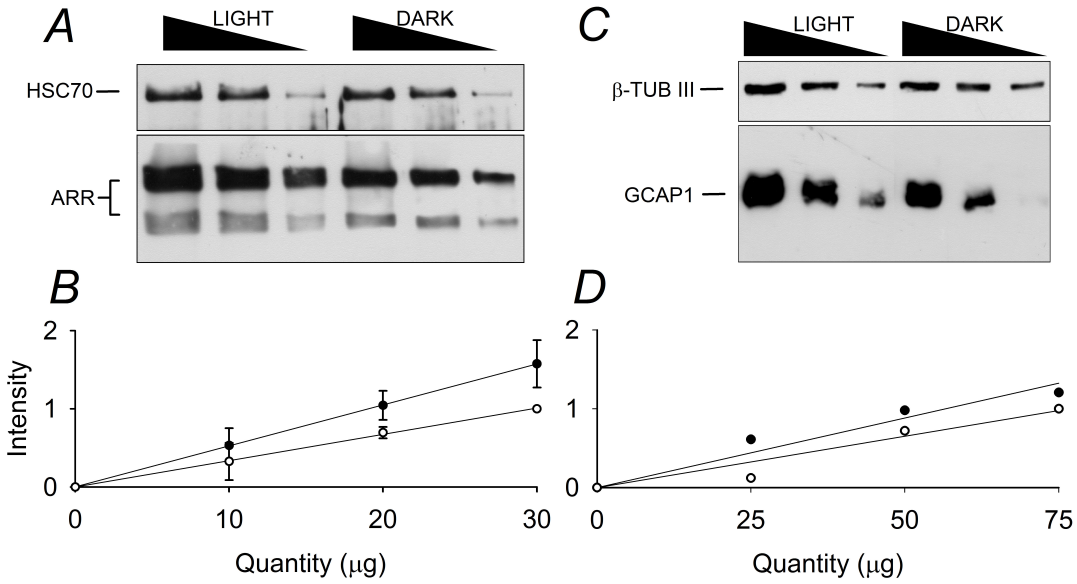


**Figure 3.9: Western blot analysis in retinas from freely moving mice** - (A) Representative Western Blot quantifying the expression of the two isoforms of arrestin protein (48kDa and 44kDa) in retinal homogenates of light (3 hours of exposure) or dark-exposed mice retinas. For each line, 30, 20 and 10 $\mu$g of the total protein was loaded. HSC70 was used as housekeeping gene control. (B) The relative increase of arrestin in light-exposed mice, calculated as the ratio of the slopes of light and dark-exposed (filled and open symbols respectively) mice, was 1.57-fold (n=3; mean±SEM). (C) Same conditions as described above, representative Western Blot quantifying the expression of GCAP1 in retinal homogenates. For each line, 75, 50 and 25 $\mu$g of the total protein was loaded. $\beta$-tubulin III was used as housekeeping gene control. (D) The relative increase of GCAP1 in light-exposed mice was 1.36-fold (n=1).

## 3.4 Real-time PCR analysis for selected genes in other systems

### 3.4.1 Real-time PCR analysis in retinas from freely moving rats

In order to extend the observation to another species we repeated similar experiments in rats, where electroretinographic tests (ERG) are easier to perform over long periods of time (see next section). As in mice, up-regulation of *Sag*, *Guca1a* and *Guca1b* expression in the rat retina was observed 2 hours after onset of light exposure ($p<0.05$; Figure 3.10A).

The increased levels of mRNAs described in Figure 3.3 and Figure 3.6 could be due to an increased rate of transcription or to a decrease of the degradation of those mRNAs. To distinguish between these two possibilities, we quantified the levels of unspliced transcripts of *Sag*, *Guca1a* and *Guca1b* as an estimate of new RNA synthesis. As shown in Figure 3.10B, the levels of these transcripts containing intron 1 of each gene increased by approximately 1.4-fold after 2 hours of light exposure, indicating that the observed increases in mRNA are caused by higher rates of transcription.

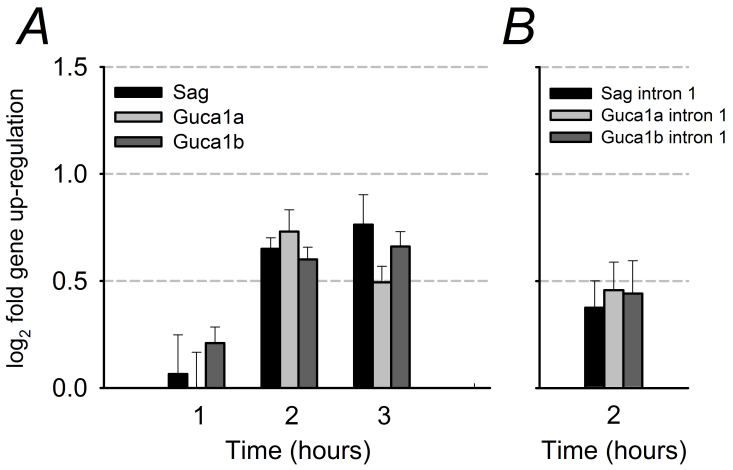


**Figure 3.10: Real time PCR analysis in retinas from freely moving rats** - (A) Time course of changes in expression (relative to the control level in dark conditions) induced by light of *Sag*, *Guca1a* and *Guca1b* genes in retinas from freely moving rats exposed to an ambient light of 1000 lux (n=6; mean±SEM). (B) Changes of unspliced *Sag*, *Guca1a* and *Guca1b* transcripts in rats after a 2-hour light exposure, detected by primers matching the intron 1 region (n=5; mean±SEM).

### 3.4.2 Real-time PCR analysis in organotypic mouse culture and in acute rat retina system

Having established the up-regulation of *Sag*, *Guca1a* and *Guca1b* expression following light exposure in freely moving mice and rats, we decided to confirm these observations in more controlled light intensity conditions. Therefore, we cultured mouse retinas as described by Reidel et al., 2006 (103). Retinas from P21 mice were explanted and cultured for two days. The left retina from each mouse was kept in the dark and used as control, whereas the right retina was exposed to a steady monochromatic light ($\lambda$=520 nm) with an intensity estimated (104; 115) to correspond to $5 \times 10^3$, $2.5 \times 10^4$ and $1 \times 10^5$ Rh$^*$/sec/rod. As shown in Figure 3.11, after 2 hours of illumination, a clear and statistically significant up-regulation ($p<0.05$) of *Sag*, *Guca1a* and *Guca1b* was observed.

Later on, we extended the intensity-dependence relation using the same strain and age of animals used for ERG recordings. These retinas were isolated from adult Long Evans rats under dim red light and prepared for culturing as described for the mouse organotypic culture. Retinas were dark-adapted for two hours and than exposed to the same light intensities used during ERG experiments, equivalent to 410 and 2000 Rh$^*$/sec/rod. The light intensity causing approximately half maximal gene up-regulation was about $5 \times 10^3$ Rh$^*$/sec/rod (see figure 3.11).

This level of light is whitin the range of light intensities initiating arrestin translocation from the inner to the outer segment (115).

## 3.5 Viability test

To confirm the good health condition of our retinal culture system and to avoid noise from light-induced photoreceptor degeneration, we performed TUNEL assay on organotypic culture. After 2 days of culturing at $1 \times 10^5$ Rh$^*$/rod/sec light intensity, the assay detected very few apoptotic nuclei (less than 5%) as shown in Fig. 3.12

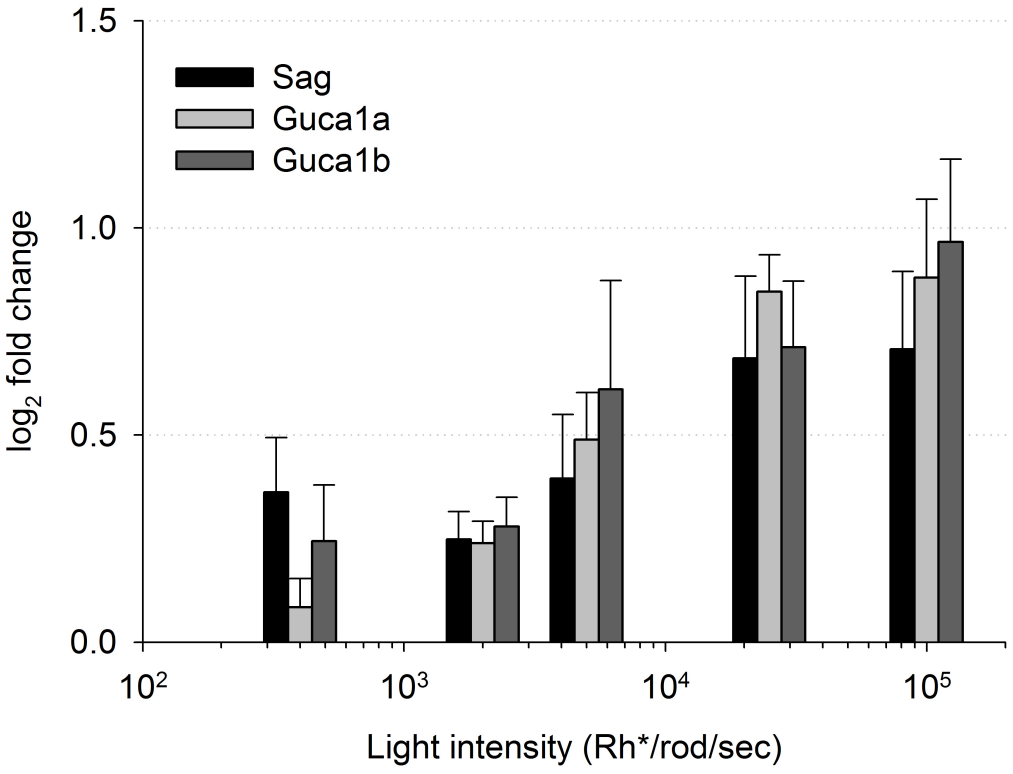


**Figure 3.11: Real time PCR analysis in mouse organotypic culture and acute rat retinas:** - Up-regulation of *Sag*, *Guca1a* and *Guca1b* after two hours of exposure to a steady light equivalent to 410 and 2000 Rh*/sec/rod in acute rat retinas and 5000, 25000 and 100000 Rh*/sec/rod in organotypic mouse retinas (n=3; mean±SEM).

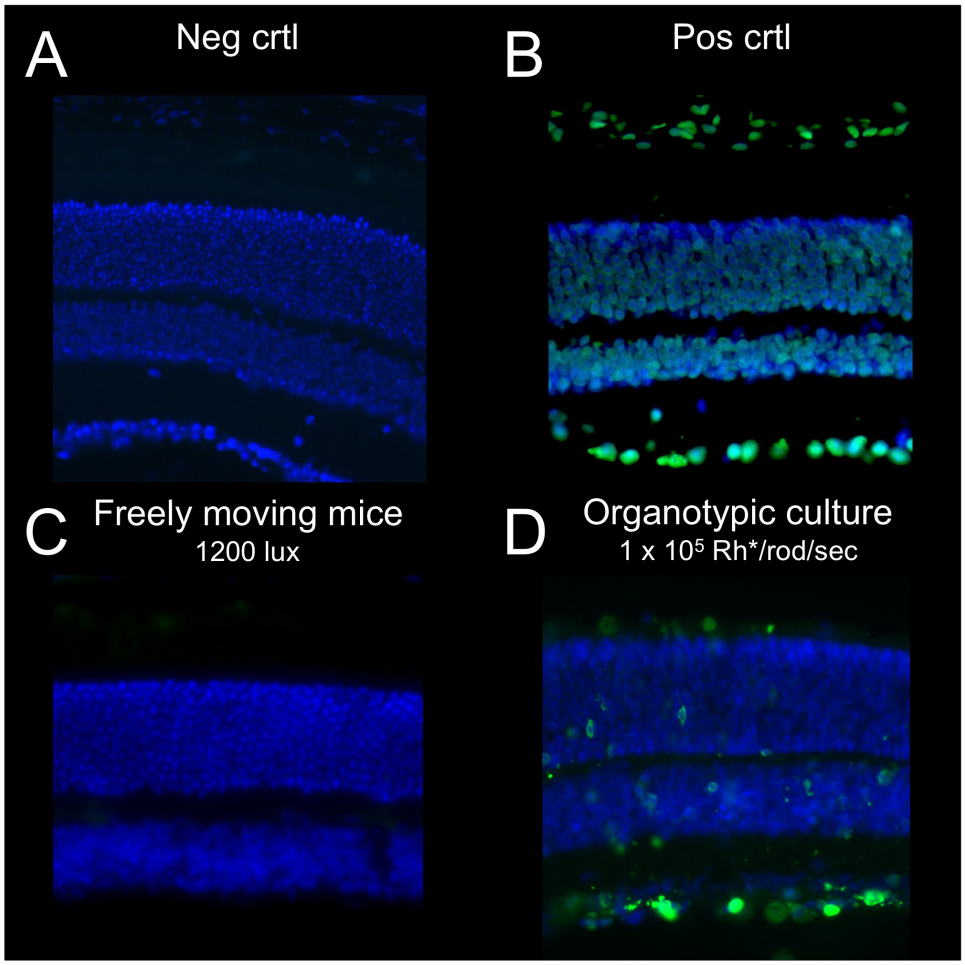


**Figure 3.12: TUNEL assay on retinas harvested from freely moving mice and on retinal cultures** - A: Negative control; B: Positive control, treated with DNase to create nicks in the genomic DNA; C: Apoptotic cells in retinas harvested from freely moving mice after 2 hours of 1200 lux illumination; D: Apoptotic cells in retinal culture, after 2 days of culturing at $1 \times 10^5$ Rh*/rod/sec light intensity

## 3.6 Analysis of late light adaptation in intact rats by ERG

The previously presented results show that exposure to a steady light equivalent to about $10^4$-$10^5$ Rh*/rod/sec causes a two-fold up-regulation of expression of genes coding for arrestin and for the two activators of guanylate cyclase and the protein concentration of arrestin and GCAP1 increases by about 40-50% (Figures 3.11 and 3.9). The up-regulation of these proteins is expected to reactivate the photocurrent and consequently to mediate a late phase of light adaptation. Therefore, we investigated the possible reactivation of the photocurrent in vivo by electroretinographic tests (ERG), following a long exposure to a steady light with a time course that was consistent with the changes in gene expression observed in Figures 3.6 and 3.10A.

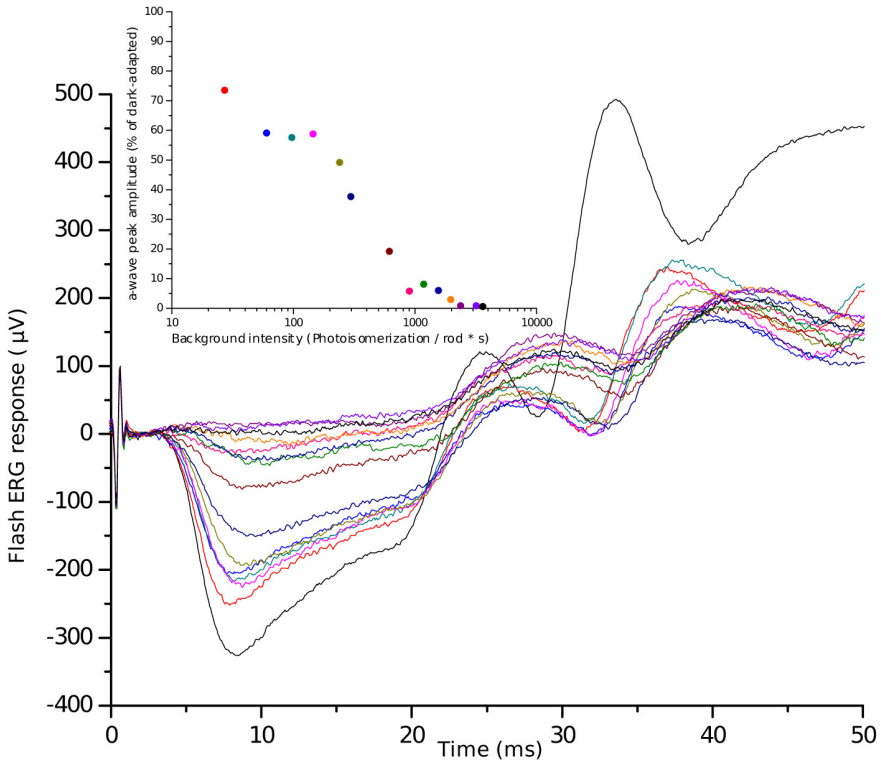


**Figure 3.13: a-wave suppression recorded increasing background light intensity in a calibration experiment** - After the recording of a dark-adapted response (black trace), background lights with an increasing intensity were applied. Each background was held for 10 minutes before the recording of the flash photoresponse (coloured traces). The recorded ERG have been superimposed starting from 0 $\mu$V.

Initial results from ERG recordings on mice were encouraging but it was very difficult to keep the animal alive throughout experiments lasting for more that five hours. For this reason, we decided to use rats as they tolerate these experimental conditions better. This is possible because gene up-regulation occuring after prolonged illumination was also observed in rats as described in the previous section (see Figures 3.10 and 3.11).

The relation between steady light intensity measured in Rh*/rod/sec and fractional suppressed photocurrent in rat rods was obtained from ERG recordings in which the amplitude of the a-wave evoked by a bright flash of light (equivalent to $1.4 \times 10^5$ Rh*/rod/sec) was measured in the presence of steady lights of increasing intensity. From these experiments we derived the relation between fractional suppressed rod photocurrent and steady light intensity (see Figure 3.13). This relation was used to determine the range of light intensity where to study light adaptation in rods, which falls between 20 and 2000 Rh*/rod/sec.

After prolonged illumination, an increased translation of arrestin and of proteins activating guanylate cyclase would be expected to result in a detectable reactivation of the circulating photocurrent. Indeed, when both eyes of a rat were exposed to steady lights equivalent to 60, 410 and 2000 Rh*/sec/rod, the amplitude of the a-wave of the ERG to a test flash delivering approximately $1.4 \times 10^5$ Rh*/rod was initially suppressed by ∼30%, ∼70% and ∼90% respectively. However, a substantial recovery was observed over the next 2-4 hours, as described in the reported representative experiments in Figures 3.15, 3.16, 3.17, 3.18 and 3.19.

The amplitude of the a-wave in dark adapted conditions (data from 5 animals), slightly decreased during experimental sessions lasting longer than 4 hours up to 80±8% of its initial value, as shown in Figure 3.14 with square symbols. In contrast, in the presence of a steady background lights, the amplitude of the a-wave, after its initial decrease, progressively increased during the experiment, as shown in Figure 3.14 and in table 3.1.

ERG recordings lasted several hours and therefore we analyzed the stability of the several components of the recording system. Fluctuations of the light intensity emitted by the diodes illuminating the rat eyes during the entire experiment were less than 13%. We also verified that modifications of the measured circulating photocurrent were not caused by changes in the electrical contacts of the recording electrodes and that the

**Table 3.1:** Averaged peak amplitude in ERG experiments

| light intensity (Rh*/r/s) | initial a-wave peak (%) | final a-wave peak (%) | fold change (final/initial) |
|---|---|---|---|
| no background | 100% | 80±8% | 0.8±0.08 |
| 60 | 66±3% | 77±5% | 1.17±0.08 |
| 410 | 32±6% | 50±5% | 1.56±0.16 |
| 2000 | 8±2% | 19±3% | 2.38±0.38 |

pupil size did not change during the experiments. Therefore, the recovery of the amplitude of the a-wave cannot be ascribed to changes of the background light intensity falling onto rod photoreceptors. Therefore, following a steady light that initially decreased the circulating photocurrent by ∼30%, ∼70% and ∼90%, a partial recovery in the photocurrent was observed after 1-2 hours.

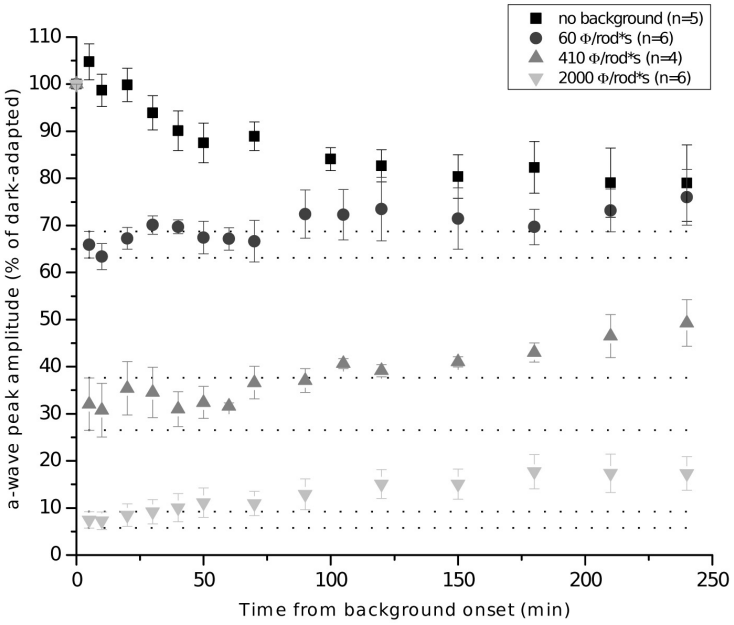


**Figure 3.14: ERG recordings in rats** - Averaged peak amplitude of a-wave as a function of time without any background (squares, n=5) or with backgrounds of light corresponding to 60 Rh*/rod/sec (circles, n=5), to 410 Rh*/rod/sec (triangles, n=5) and to 2000 Rh*/rod/sec (inverted triangles, n=6). For values see table 3.1

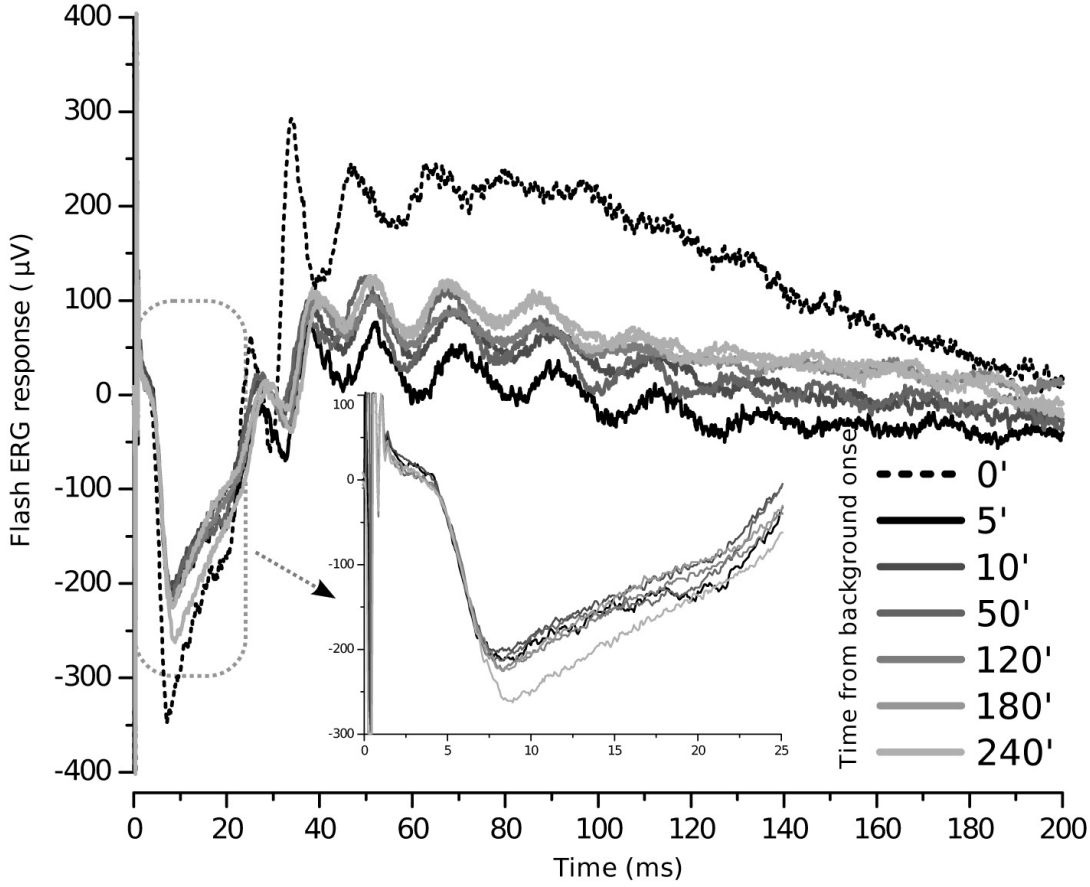


**Figure 3.15: ERG recordings in rats** - ERG in dark adapted conditions in response to a bright flash of light delivering $1.4 \times 10^5$ Rh$^*$/rod (dotted curve), immediately after the onset of a steady light corresponding to 60 Rh$^*$/rod/sec (black curve) and at later times (shaded grey curves). The amplitude of the a-wave, which was 346 $\mu$V in dark-adapted conditions, immediately decreased to 213 $\mu$V (61% of the dark-adapted response) upon the onset of the background light. While the background light was maintained, the amplitude of the a-wave slowly recovered, so that after 240 minutes it was approximately 261 $\mu$V, about 75% of its value in the dark-adapted conditions. The inset reproduces the ERG responses in the dotted box.

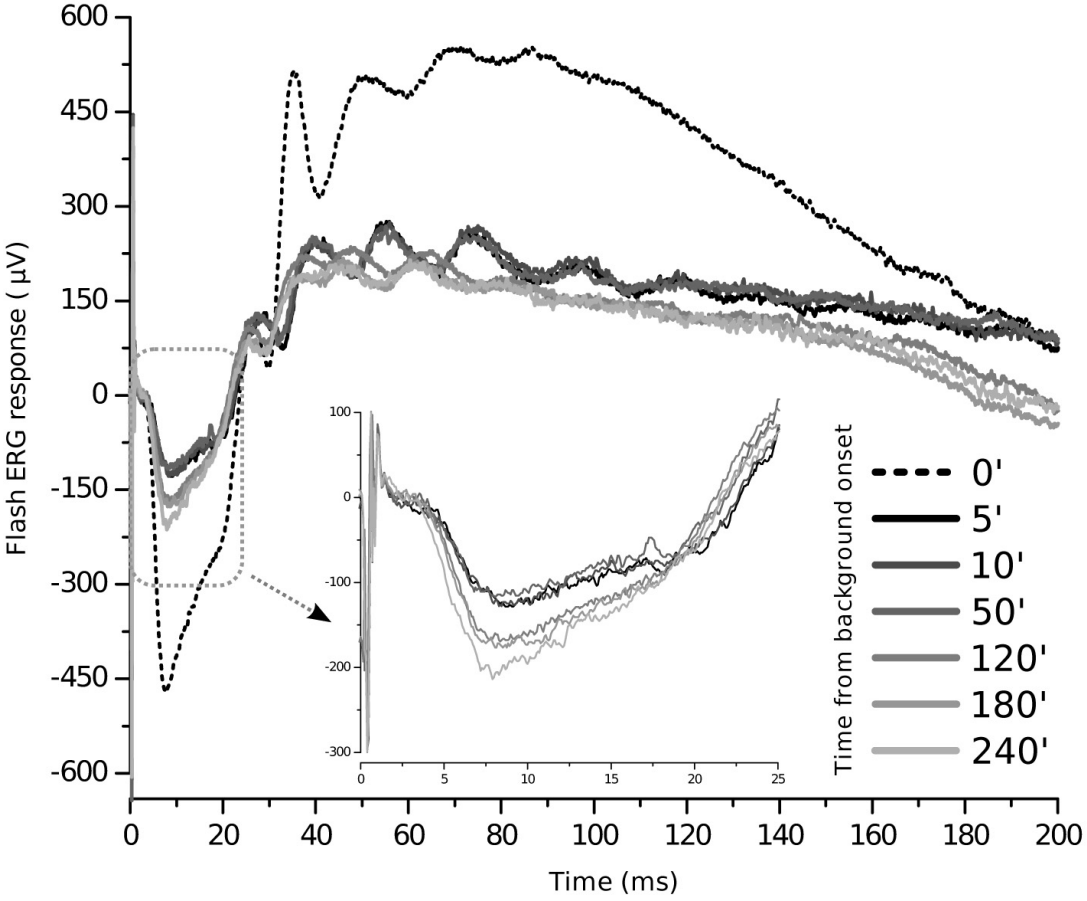


**Figure 3.16: ERG recordings in rats** - ERG in dark adapted conditions in response to a bright flash of light delivering $1.4 \times 10^5$ Rh*/rod (dotted curve), immediately after the onset of a steady light corresponding to 410 Rh*/rod/sec (black curve) and at later times (shaded grey curves). The amplitude of the a-wave, which was 463 $\mu$V in dark-adapted conditions, immediately decreased to 124 $\mu$V (27% of the dark-adapted response) upon the onset of the background light. While the background light was maintained, the amplitude of the a-wave slowly recovered, so that after 240 minutes it was approximately 212 $\mu$V, about 46% of its value in the dark-adapted conditions. The inset reproduces the ERG responses in the dotted box.

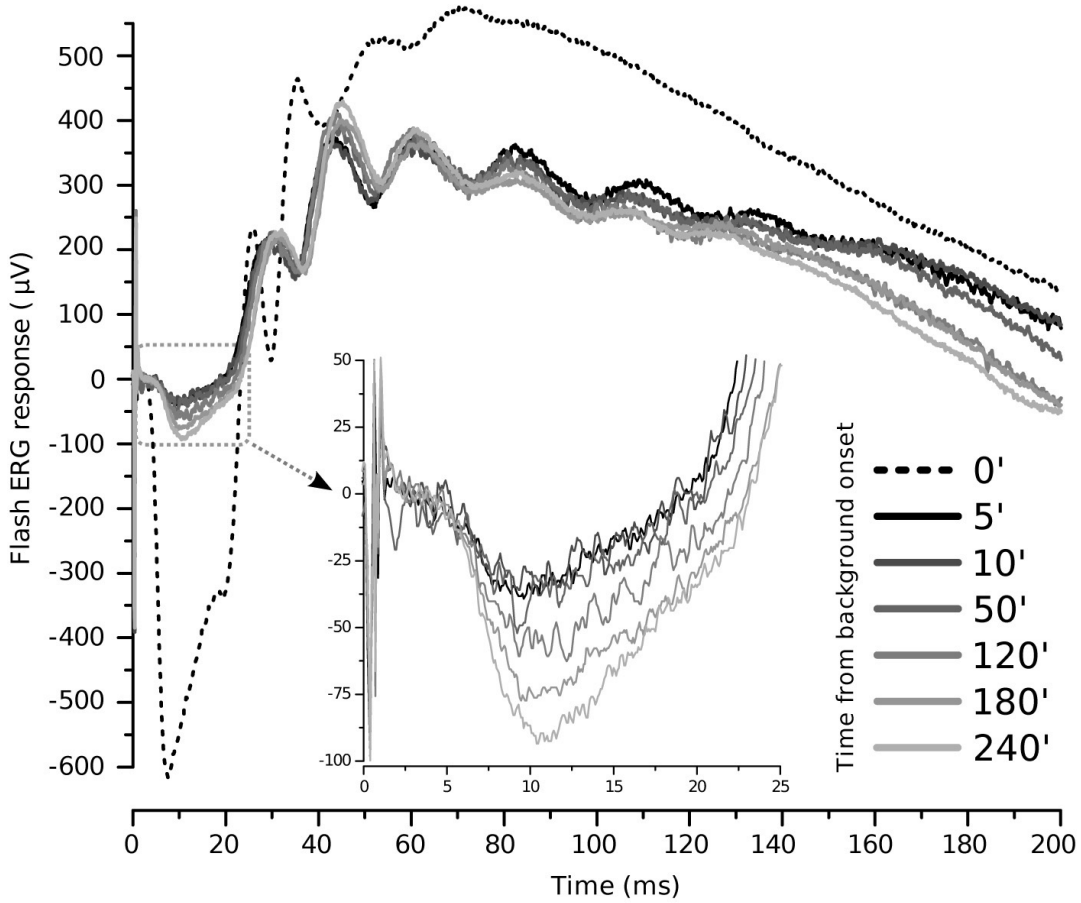


**Figure 3.17: ERG recordings in rats** - ERG in dark adapted conditions in response to a bright flash of light delivering $1.4 \times 10^5$ Rh$^*$/rod (dotted curve), immediately after the onset of a steady light corresponding to 2000 Rh$^*$/rod/sec (black curve) and at later times (shaded grey curves). The amplitude of the a-wave, which was 628 $\mu$V in dark-adapted conditions, immediately decreased to 38 $\mu$V (6% of the dark-adapted response) upon the onset of the background light. While the background light was maintained, the amplitude of the a-wave slowly recovered, so that after 240 minutes it was approximately 91 $\mu$V, about 15% of its value in the dark-adapted conditions. The inset reproduces the ERG responses in the dotted box.

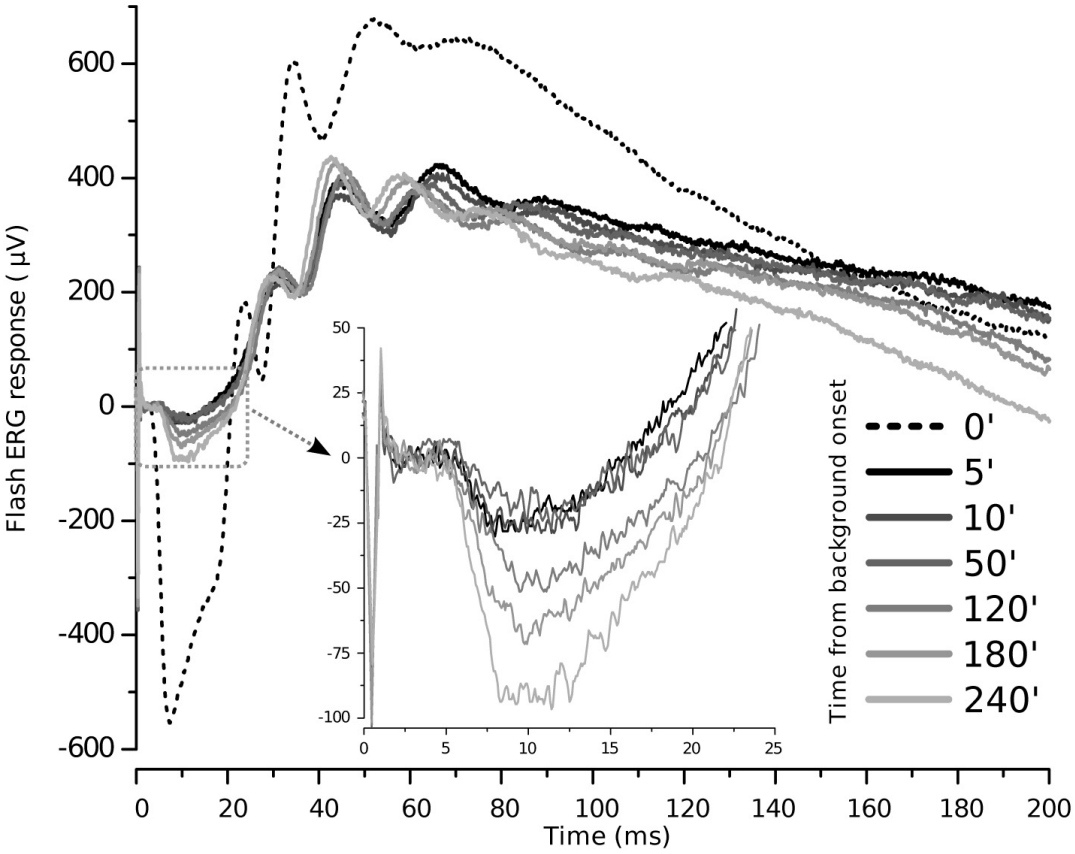


**Figure 3.18: ERG recordings in rats** - ERG in dark adapted conditions in response to a bright flash of light delivering $1.4 \times 10^5$ Rh*/rod (dotted curve), immediately after the onset of a steady light corresponding to 2000 Rh*/rod/sec (black curve) and at later times (shaded grey curves). The amplitude of the a-wave, which was 553 $\mu$V in dark-adapted conditions, immediately decreased to 26 $\mu$V (about 5% of the dark-adapted response) upon the onset of the background light. While the background light was maintained, the amplitude of the a-wave slowly recovered, so that after 240 minutes it was approximately 92 $\mu$V, about 17% of its value in the dark-adapted conditions. The inset reproduces the ERG responses in the dotted box.

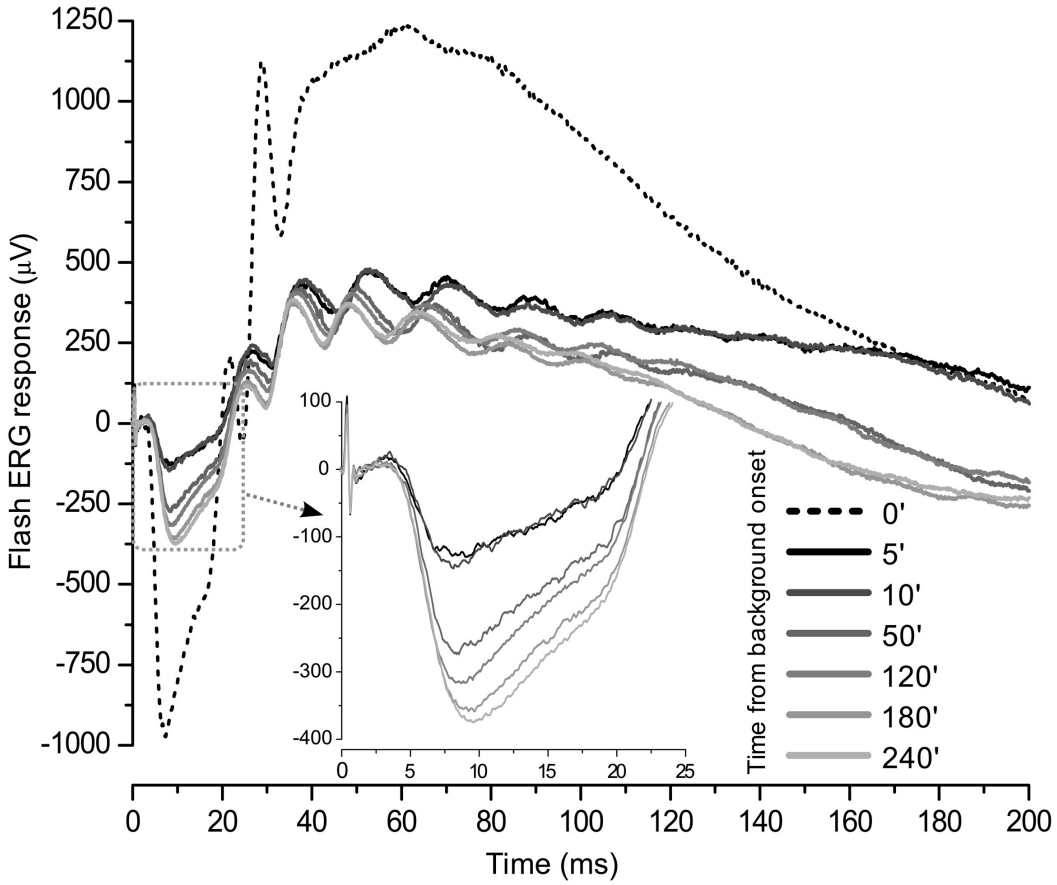


**Figure 3.19: ERG recordings in rats** - ERG in dark adapted conditions in response to a bright flash of light delivering $1.4 \times 10^5$ Rh$^*$/rod (dotted curve), immediately after the onset of a steady light corresponding to 2000 Rh$^*$/rod/sec (black curve) and at later times (shaded grey curves). The amplitude of the a-wave, which was 970 $\mu$V in dark-adapted conditions, immediately decreased to 125 $\mu$V (about 13% of the dark-adapted response) upon the onset of the background light. While the background light was maintained, the amplitude of the a-wave slowly recovered, so that after 240 minutes it was approximately 360 $\mu$V, nearly 38% of its value in the dark-adapted conditions. The inset reproduces the ERG responses in the dotted box.

# 4

# Discussion

The range of light intensity that we encounter daily spans more than ten orders of magnitude and this requires the photoreceptor system to constantly optimize their sensitivity through a process known as light adaptation. Light adaptation is mediated by many mechanisms, some of them depend on the intracellular fall of $Ca^{2+}$ (9; 13; 27; 48; 54; 63; 74; 96; 120), others are related to the modification of enzyme efficiency (23; 86; 87) or to protein translocation (110). Even if this topic has been a matter of study for more than two decades, the genomic contribution to light adaptation mechanisms has never been studied before.

For this reason, I investigated on whether light could influence and regulate the expression of genes involved in phototransduction and whether this regulation could influence the photoresponse.

The work done for this thesis provides experimental evidence for a role of changes in gene expression in light adaptation following exposures to steady light for longer than 1-2 hours with an intensity corresponding to a range between $4 \times 10^2$ and $10^5$ $Rh^*$/rod/sec. An up-regulation of genes coding for arrestin and the two activators of guanylate cyclase was observed in three different rodent preparations. *In vivo* ERG recordings from rats indicate that following a prolonged exposure to steady lights, that initially suppressed ∼30%, ∼70% and ∼90% of the circulating photocurrent, a partial recovery of this photocurrent is observed after 1-2 hours. These results identify a novel component of light adaptation possibly associated to changes of gene expression.

Up-regulation of *Sag* and *Guca1a* expression was initially observed in groups of rod photoreceptors dissociated from mouse retinas (Figures 3.1, 3.3 and 3.4) by microarray

screening. As dissociated photoreceptors usually exhibit signs of degeneration following a prolonged steady light, we could not investigate the effect of light exposure for longer than 2 hours. In order to study this effect over a longer period, we decided to perform the experiments on freely moving mice and rats. Retinas from these animals did not show any sign of photoreceptor deterioration (Figure 3.12) and the initial observation of a significant up-regulation of *Sag*, *Guca1a* and *Guca1b* expression was also found in these preparations (Figures 3.6 and 3.10). *Sag*, *Guca1a* and *Guca1b* genes were found to be up-regulated by nearly two-fold in mice exposed to light for a time period longer than 2 hours and remained high for 12 hours. Moreover, this up-regulation showed intensity-dependent characteristics (Figures 3.7 and 3.11). The health and integrity of retinas in freely moving mice and rats is normal for the range of the ambient light used, but under those conditions, it is not possible to accurately control the flux of light impinging on rod photoreceptors. Therefore, we studied whether the light-dependent gene expression changes observed in vivo also took place in explanted retinas. These retinas generally survive for several days and exhibit the typical physiological arrestin and transducin migration (103). Up-regulation of *Sag*, *Guca1a* and *Guca1b* expression was also observed in explanted retinal cultures in the presence of steady lights in a range between $4 \times 10^2$ and $10^5$ $Rh^*$/rod/sec (Figures 3.7 and 3.11).

To verify whether up-regulation of *Sag*, *Guca1a* and *Guca1b* genes leads to an increased translation of proteins, we analyzed the levels of arrestin and GCAP1 by Western Blot assay. Unfortunately, we were not able to analyze the GCAP2 levels due to the lack of a reliable commercial antibody. Western blot analysis determined that the quantity of arrestin, extracted from retinal homogenates, increased by 57% and the quantity of GCAP1 by 36% after 3 hours of 1000 lux ambient light exposure (Figure 3.9).

Arrestin is a cytosolic protein, known to block the interaction between rhodopsin and transducin (66; 122; 128) playing a key role on the two-step process for activated rhodopsin shut-off. Activated rhodopsin is multi-phosphorilated by rhodopsin kinase and this allows arrestin to bind with rhodopsin, preventing further activation of transducin by steric hindrance. In experiments with knock-out mice for arrestin (128), the kinetics of the photoresponse is almost unchanged in +/- heterozygous mice, suggesting that a decrease of the concentration of arrestin by 1/2 does not affect the kinetics of photoresponses. Indeed the kinetics of photoresponses to brief light flashes is primarily controlled by Regulators of G protein signaling (64) and not by arrestin. However,

in w.t. mice, the ratio between rhodopsin and arrestin molecules is 8 to 1 (70) and when prolonged bright lights activate a considerable number of rhodopsin molecules, an higher level of arrestin protein is expected to lead to a more effective shutting-off of activated Rh* and therefore to a partial reactivation of the photocurrent.

GCAPs are $Ca^{2+}$-binding proteins, known to stimulate guanyl cyclases in the $Ca^{2+}$-free form and inhibit GCs upon $Ca^{2+}$ binding (79; 94). The $Ca^{2+}$/GCAP-dependent regulation of guanylate cyclase activity forms a powerful feedback mechanism in which the rate of cGMP synthesis increases as $Ca^{2+}$ concentration drops during photoresponse. In vitro studies show that GC activity depends on the GCAP1 concentration (127) and it has been calculated that $EC_{50}$ for GCAP1 to be around 1 $\mu$M and for GCAP2 to be around 6 $\mu$M (99), while the GC density in mammalian rod membrane is 50 $\mu m^{-2}$, corresponding to $2 \times 10^5$ GC molecules per rod (101). Similarly, the estimated number of GCAP1 and GCAP2 molecules per rod is in the range of $2 \times 10^4$ and $1 \times 10^5$, respectively. Therefore GC molecules are not completely covered by GCAPs and consequently an increase in GCAPs concentration is expected to lead to GC activitation. Moreover, GCAPs +/- mice that express approximately half the normal levels of GCAP1 and GCAP2 show a delayed kinetics of phototesponses: an intermediate state between knockout and wild-type rods (79). According to these considerations, a change in the cytoplasmic concentration of the GCAP1 (coded by *Guca1a*) and GCAP2 (coded by *Guca1b*) proteins is expected to lead to a modification in the GC activity and consequently to a partial reactivation of the circulating photocurrent.

Therefore, up-regulation expression of *Sag*, *Guca1a* and *Guca1b* could be a novel form of light adaptation occurring over a time scale of several hours, possibly underlying the recovery of the a-wave amplitude observed *in vivo*.

The *in vivo* ERG recordings from rats show that the circulating photocurrent, initially suppressed by the background light, reactivates significantly after 1-2 hours (Fig. 3.14). The amplitude of the a-wave was initially suppressed by ∼30%, ∼70% and ∼90% in the presence of different steady backgrounds of light but showed subsequently a recovery of 1.17±0.08-fold, 1.56±0.16-fold and 2.38±0.38-fold, respectively. The possibility that the observed reactivation of the photocurrent may be due to a progressive closure of the animal pupil, leading to a decrease of the amount of light impinging on photoreceptors, was ruled out by pupil size measurements that found no significant changes over the

entire experimental session. Therefore, we conclude that the observed reactivation of the photocurrent is a genuine effect.

The signaling pathway by which light regulates transcription of these genes in rod photoreceptors is currently unknown. The decrease of intracellular $Ca^{2+}$ occurring during light adaptation (19; 20; 36; 63; 100; 120) is a potential part of this signaling pathway, but the combination of different experimental techniques will be required to unravel this new pathway of phototransduction.

Our experimental results show that the effect of light in visual photoreceptors is not limited to events occurring in the cytoplasm, but acts also in the nucleus by regulating transcription. Finally, it can be concluded that the transcriptional control of visual transduction in rods and cones is a novel finding and describes a previously unappreciated level of control of this process.

# References


[1] G Abdulaeva, P A Hargrave, and W C Smith. **The sequence of arrestins from rod and cone photoreceptors in the frogs Rana catesbeiana and Rana pipiens. Localization of gene transcripts by reverse-transcription polymerase chain reaction on isolated photoreceptors.** *Eur J Biochem*, **234**(2):437–442, 1995. 19

[2] Vadim Y Arshavsky. **Rhodopsin phosphorylation: from terminating single photon responses to photoreceptor dark adaptation.** *Trends Neurosci*, **25**(3):124–126, 2002. 18

[3] Vadim Y Arshavsky, Trevor D Lamb, and Edward N Jr Pugh. **G proteins and phototransduction.** *Annu Rev Physiol*, **64**:153–187, 2002. 16

[4] N O Artemyev, M Natochin, M Busman, K L Schey, and H E Hamm. **Mechanism of photoreceptor cGMP phosphodiesterase inhibition by its gamma-subunits.** *Proc Natl Acad Sci U S A*, **93**(11):5407–5412, 1996. 20

[5] H Attramadal, J L Arriza, C Aoki, T M Dawson, J Codina, M M Kwatra, S H Snyder, M G Caron, and R J Lefkowitz. **Beta-arrestin2, a novel member of the arrestin/beta-arrestin gene family.** *J Biol Chem*, **267**(25):17882–17890, 1992. 19

[6] Wolfgang Baehr, Sukanya Karan, Tadao Maeda, Dong-Gen Luo, Sha Li, J Darin Bronson, Carl B Watt, King-Wai Yau, Jeanne M Frederick, and Krzysztof Palczewski. **The function of guanylate cyclase 1 and guanylate cyclase 2 in rod and cone photoreceptors.** *J Biol Chem*, **282**(12):8837–8847, 2007. 20

[7] S Barattini, B Battisti, L Cervetto, and P Marroni. **Diurnal changes in the pigeon electroretinogram.** *Rev Can Biol*, **40**(1):133–137, 1981. 34

[8] Alun R Barnard, Samer Hattar, Mark W Hankins, and Robert J Lucas. **Melanopsin regulates visual processing in the mouse retina.** *Curr Biol*, **16**(4):389–395, 2006. 34

[9] P J Bauer. **Cyclic GMP-gated channels of bovine rod photoreceptors: affinity, density and stoichiometry of Ca(2+)-calmodulin binding sites.** *J Physiol*, **494 ( Pt 3)**:675–685, 1996. 23, 63

[10] D A Baylor, M G Fuortes, and P M O'Bryan. **Receptive fields of cones in the retina of the turtle.** *J Physiol*, **214**(2):265–294, 1971. 6

[11] D A Baylor, G Matthews, and K W Yau. **Two components of electrical dark noise in toad retinal rod outer segments.** *J Physiol*, **309**:591–621, 1980. 22

[12] N Berardi, L Domenici, A Gravina, and L Maffei. **Pattern ERG in rats following section of the optic nerve.** *Exp Brain Res*, **79**(3):539–546, 1990. 33

[13] M S Biernbaum and M D Bownds. **Influence of light and calcium on guanosine 5'-triphosphate in isolated frog rod outer segments.** *J Gen Physiol*, **74**(6):649–669, 1979. 22, 63

[14] S Blackshaw and S H Snyder. **Developmental expression pattern of phototransduction components in mammalian pineal implies a light-sensing function.** *J Neurosci*, **17**(21):8074–8082, 1997. 19

[15] Kendall J Blumer. **Vision: the need for speed.** *Nature*, **427**(6969):20–21, 2004. 20

[16] C Bowes, T van Veen, and D B Farber. **Opsin, G-protein and 48-kDa protein in normal and rd mouse retinas: developmental expression of mRNAs and proteins and light/dark cycling of mRNAs.** *Exp Eye Res*, **47**(3):369–390, 1988. 19

[17] D Bownds, J Dawes, J Miller, and M Stahlman. **Phosphorylation of frog photoreceptor membranes induced by light.** *Nat New Biol*, **237**(73):125–127, 1972. 10

[18] M L Breitman, M Tsuda, J Usukura, T Kikuchi, A Zucconi, W Khoo, and T Shinohara. **Expression of S-antigen in retina, pineal gland, lens, and brain is directed by 5'-flanking sequences.** *J Biol Chem*, **266**(23):15505–15510, 1991. 19

[19] M E Burns and D A Baylor. **Activation, deactivation, and adaptation in vertebrate photoreceptor cells.** *Annu Rev Neurosci*, **24**:779–805, 2001. 15, 66

[20] Marie E Burns and Vadim Y Arshavsky. **Beyond counting photons: trials and trends in vertebrate visual transduction.** *Neuron*, **48**(3):387–401, 2005. 11, 17, 66

[21] Marie E Burns, Ana Mendez, Jeannie Chen, and Denis A Baylor. **Dynamics of cyclic GMP synthesis in retinal rods.** *Neuron*, **36**(1):81–91, 2002. 21, 22

[22] P D Calvert, V A Klenchin, and M D Bownds. **Rhodopsin kinase inhibition by recoverin. Function of recoverin myristoylation.** *J Biol Chem*, **270**(41):24127–24129, 1995. 18

[23] Peter D Calvert, Victor I Govardovskii, Vadim Y Arshavsky, and Clint L Makino. **Two temporal phases of light adaptation in retinal rods.** *J Gen Physiol*, **119**(2):129–145, 2002. 23, 63

[24] P Catty and P Deterre. **Activation and solubilization of the retinal cGMP-specific phosphodiesterase by limited proteolysis. Role of the C-terminal domain of the beta-subunit.** *Eur J Biochem*, **199**(2):263–269, 1991. 15

[25] P Catty, C Pfister, F Bruckert, and P Deterre. **The cGMP phosphodiesterase-transducin complex of retinal rods. Membrane binding and subunits interactions.** *J Biol Chem*, **267**(27):19489–19493, 1992. 15

[26] C K Chen, M E Burns, M Spencer, G A Niemi, J Chen, J B Hurley, D A Baylor, and M I Simon. **Abnormal photoresponses and light-induced apoptosis in rods lacking rhodopsin kinase.** *Proc Natl Acad Sci U S A*, **96**(7):3718–3722, 1999. 18

[27] C K Chen, J Inglese, R J Lefkowitz, and J B Hurley. **Ca(2+)-dependent interaction of recoverin with rhodopsin kinase.** *J Biol Chem*, **270**(30):18060–18066, 1995. 18, 22, 63

[28] J Chen, C L Makino, N S Peachey, D A Baylor, and M I Simon. **Mechanisms of rhodopsin inactivation in vivo as revealed by a COOH-terminal truncation mutant.** *Science*, **267**(5196):374–377, 1995. 17

[29] H Coles. **Nobel honours pursuit of G proteins.** *Nature*, **371**(6498):547, 1994. 13

[30] C M Craft and D H Whitmore. **The arrestin superfamily: cone arrestins are a fourth family.** *FEBS Lett*, **362**(2):247–255, 1995. 19

[31] C M Craft, D H Whitmore, and A F Wiechmann. **Cone arrestin identified by targeting expression of a functional family.** *J Biol Chem*, **269**(6):4613–4619, 1994. 19

[32] L J Croner and E Kaplan. **Receptive fields of P and M ganglion cells across the primate retina.** *Vision Res*, **35**(1):7–24, 1995. 9

[33] S H DeVries and D A Baylor. **Synaptic circuitry of the retina and olfactory bulb.** *Cell*, **72 Suppl**:139–149, 1993. 6

[34] A M Dizhoor, E V Olshevskaya, W J Henzel, S C Wong, J T Stults, I Ankoudinova, and J B Hurley. **Cloning, sequencing, and expression of a 24-kDa Ca(2+)-binding protein activating photoreceptor guanylyl cyclase.** *J Biol Chem*, **270**(42):25200–25206, 1995. 21

[35] Rajesh V Elias, Steven S Sezate, Wei Cao, and James F McGinnis. **Temporal kinetics of the light/dark translocation and compartmentation of arrestin and alpha-transducin in mouse photoreceptor cells.** *Mol Vis*, **10**:672–681, 2004. 24, 25

[36] G L Fain, H R Matthews, M C Cornwall, and Y Koutalos. **Adaptation in vertebrate photoreceptors.** *Physiol Rev*, **81**(1):117–151, 2001. 66

[37] S S Ferguson, L S Barak, J Zhang, and M G Caron. **G-protein-coupled receptor regulation: role of G-protein-coupled receptor kinases and arrestins.** *Can J Physiol Pharmacol*, **74**(10):1095–1110, 1996. 19

[38] E E Fesenko, S S Kolesnikov, and A L Lyubarsky. **Induction by cyclic GMP of cationic conductance in plasma membrane of retinal rod outer segment.** *Nature*, **313**(6000):310–313, 1985. 10

[39] S Fuchs, M Nakazawa, M Maw, M Tamai, Y Oguchi, and A Gal. **A homozygous 1-base pair deletion in the arrestin gene is a frequent cause of Oguchi disease in Japanese.** *Nat Genet*, **10**(3):360–362, 1995. 19

[40] Y Fukada, T Matsuda, K Kokame, T Takao, Y Shimonishi, T Akino, and T Yoshizawa. **Effects of carboxyl methylation of photoreceptor G protein gamma-subunit in visual transduction.** *J Biol Chem*, **269**(7):5163–5170, 1994. 15

[41] C Gargini, S Bisti, G C Demontis, K Valter, J Stone, and L Cervetto. **Electroretinogram changes associated with retinal upregulation of trophic factors: observations following optic nerve section.** *Neuroscience*, **126**(3):775–783, 2004. 33

[42] W A Gorczyca, M P Gray-Keller, P B Detwiler, and K Palczewski. **Purification and physiological evaluation of a guanylate cyclase activating protein from retinal rods.** *Proc Natl Acad Sci U S A*, **91**(9):4014–4018, 1994. 44

[43] Peter Gouras and Bjorn Ekesten. **Why do mice have ultra-violet vision?** *Exp Eye Res*, **79**(6):887–892, 2004. 4

[44] W He, C W Cowan, and T G Wensel. **RGS9, a GTPase accelerator for phototransduction.** *Neuron*, **20**(1):95–102, 1998. 19

[45] O Hisatomi, Y Imanishi, T Satoh, and F Tokunaga. **Arrestins expressed in killifish photoreceptor cells.** *FEBS Lett*, **411**(1):12–18, 1997. 19

[46] A L Hodgkin, P A McNaughton, and B J Nunn. **Measurement of sodium-calcium exchange in salamander rods.** *J Physiol*, **391**:347–370, 1987. 21

[47] Kim A Howes, Mark E Pennesi, Izabela Sokal, Jill Church-Kopish, Ben Schmidt, David Margolis, Jeanne M Frederick, Fred Rieke, Krzysztof Palczewski, Samuel M Wu, Peter B Detwiler, and Wolfgang Baehr. **GCAP1 rescues rod photoreceptor response in GCAP1/GCAP2 knockout mice.** *EMBO J*, **21**(7):1545–1554, 2002. 21

[48] Y T Hsu and R S Molday. **Modulation of the cGMP-gated channel of rod photoreceptor cells by calmodulin.** *Nature*, **361**(6407):76–79, 1993. 23, 63

[49] Guang Hu and Theodore G Wensel. **R9AP, a membrane anchor for the photoreceptor GTPase accelerating protein, RGS9-1.** *Proc Natl Acad Sci U S A*, **99**(15):9755–9760, 2002. 19

[50] J Inglese, W J Koch, M G Caron, and R J Lefkowitz. **Isoprenylation in regulation of signal transduction by G-protein-coupled receptor kinases.** *Nature*, **359**(6391):147–150, 1992. 18

[51] H Jindrova. **Vertebrate phototransduction: activation, recovery, and adaptation.** *Physiol Res*, **47**(3):155–168, 1998. 15

[52] Eric R. Kandel, James H. Schwartz, and Thomas M. Jessell. *PRINCIPLES OF NEURAL SCIENCE*. McGraw-Hill, 2000. 6

[53] E Kaplan and R M Shapley. **The primate retina contains two types of ganglion cells, with high and low contrast sensitivity.** *Proc Natl Acad Sci U S A*, **83**(8):2755–2757, 1986. 9

[54] S Kawamura. **Rhodopsin phosphorylation as a mechanism of cyclic GMP phosphodiesterase regulation by S-modulin.** *Nature*, **362**(6423):855–857, 1993. 22, 63

[55] D J Kelleher and G L Johnson. **Characterization of rhodopsin kinase purified from bovine rod outer segments.** *J Biol Chem*, **265**(5):2632–2639, 1990. 18

[56] C K Kier, G Buchsbaum, and P Sterling. **How retinal microcircuits scale for ganglion cells of different size.** *J Neurosci*, **15**(11):7673–7683, 1995. 9

[57] K Kokame, Y Fukada, T Yoshizawa, T Takao, and Y Shimonishi. **Lipid modification at the N terminus of photoreceptor G-protein alpha-subunit.** *Nature*, **359**(6397):749–752, 1992. 15

[58] H Kolb. **Amacrine cells of the mammalian retina: neurocircuitry and functional roles.** *Eye*, **11 ( Pt 6)**:904–923, 1997. 8

[59] H Kolb and E V Famiglietti. **Rod and cone pathways in the inner plexiform layer of cat retina.** *Science*, **186**(4158):47–49, 1974. 7

[60] H Kolb, E Fernandez, J Schouten, P Ahnelt, K A Linberg, and S K Fisher. **Are there three types of horizontal cell in the human retina?** *J Comp Neurol*, **343**(3):370–386, 1994. 7

[61] H Kolb, A Mariani, and A Gallego. **A second type of horizontal cell in the monkey retina.** *J Comp Neurol*, **189**(1):31–44, 1980. 7

[62] B Korf, M D Rollag, and H W Korf. **Ontogenetic development of S-antigen- and rod-opsin immunoreactions in retinal and pineal photoreceptors of Xenopus laevis in relation to the onset of melatonin-dependent color-change mechanisms.** *Cell Tissue Res*, **258**(2):319–329, 1989. 19

[63] Y Koutalos and K W Yau. **Regulation of sensitivity in vertebrate rod photoreceptors by calcium.** *Trends Neurosci*, **19**(2):73–81, 1996. 23, 63, 66

[64] Claudia M Krispel, Desheng Chen, Nathan Melling, Yu-Jiun Chen, Kirill A Martemyanov, Nidia Quillinan, Vadim Y Arshavsky, Theodore G Wensel, Ching-Kang Chen, and Marie E Burns. **RGS expression rate-limits recovery of rod photoresponses.** *Neuron*, **51**(4):409–416, 2006. 64

[65] J G Krupnick, V V Gurevich, and J L Benovic. **Mechanism of quenching of phototransduction. Binding competition between arrestin and transducin for phosphorhodopsin.** *J Biol Chem*, **272**(29):18125–18131, 1997. 18

[66] H Kuhn. **Light-regulated binding of rhodopsin kinase and other proteins to cattle photoreceptor membranes.** *Biochemistry*, **17**(21):4389–4395, 1978. 10, 64

[67] H Kuhn and WJ Dreyer. **Light dependent phosphorylation of rhodopsin by ATP.** *FEBS Lett*, **20**(1):1–6, 1972. 10

[68] W Kuhne. **On the Stable Colours of the Retina.** *J Physiol*, **1**(2-3):109–212, 1878. 10

[69] W Kuhne. **Chemical processes in the retina.** *Vision Res*, **17**(11-12):1269–1316, 1977. 10

[70] T D Lamb and E N Jr Pugh. **Dark adaptation and the retinoid cycle of vision.** *Prog Retin Eye Res*, **23**(3):307–380, 2004. 36, 65

[71] K J Livak and T D Schmittgen. **Analysis of relative gene expression data using real-time quantitative PCR and the 2(-Delta Delta C(T)) Method.** *Methods*, **25**(4):402–408, 2001. 31

[72] A L Lyubarsky and E N Jr Pugh. **Recovery phase of the murine rod photoresponse reconstructed from electroretinographic recordings.** *J Neurosci*, **16**(2):563–571, 1996. 33

[73] M A MacNeil, J K Heussy, R F Dacheux, E Raviola, and R H Masland. **The shapes and numbers of amacrine cells: matching of photofilled with Golgi-stained cells in the rabbit retina and comparison with other mammalian species.** *J Comp Neurol*, **413**(2):305–326, 1999. 8

[74] Clint L Makino, R L Dodd, J Chen, M E Burns, A Roca, M I Simon, and D A Baylor. **Recoverin regulates light-dependent phosphodiesterase activity in retinal rods.** *J Gen Physiol*, **123**(6):729–741, 2004. 23, 63

[75] E R Makino, J W Handy, T Li, and V Y Arshavsky. **The GTPase activating factor for transducin in rod photoreceptors is the complex between RGS9 and type 5 G protein beta subunit.** *Proc Natl Acad Sci U S A*, **96**(5):1947–1952, 1999. 19

[76] J Marx. **Nobel Prizes. Medicine: a signal award for discovering G proteins.** *Science*, **266**(5184):368–369, 1994. 13

[77] R H Masland. **The fundamental plan of the retina.** *Nat Neurosci*, **4**(9):877–886, 2001. 8, 9

[78] A Mendez, M E Burns, A Roca, J Lem, L W Wu, M I Simon, D A Baylor, and J Chen. **Rapid and reproducible deactivation of rhodopsin requires multiple phosphorylation sites.** *Neuron*, **28**(1):153–164, 2000. 18

[79] A Mendez, M E Burns, I Sokal, A M Dizhoor, W Baehr, K Palczewski, D A Baylor, and J Chen. **Role of guanylate cyclase-activating proteins (GCAPs) in setting the flash sensitivity of rod photoreceptors.** *Proc Natl Acad Sci U S A*, **98**(17):9948–9953, 2001. 21, 65

[80] T J Millar. **Effect of kainic acid and NMDA on the pattern electroretinogram, the scotopic threshold response, the oscillatory potentials and the electroretinogram in the urethane anaesthetized cat.** *Vision Res*, **34**(9):1111–1125, 1994. 33

[81] E M Morrow, M J Belliveau, and C L Cepko. **Two phases of rod photoreceptor differentiation during rat retinal development.** *J Neurosci*, **18**(10):3738–3748, 1998. 39

[82] K Saidas Nair, Susan M Hanson, Ana Mendez, Eugenia V Gurevich, Matthew J Kennedy, Valery I Shestopalov, Sergey A Vishnivetskiy, Jeannie Chen, James B Hurley, Vsevolod V Gurevich, and Vladlen Z Slepak.

**Light-dependent redistribution of arrestin in vertebrate rods is an energy-independent process governed by protein-protein interactions.** *Neuron*, **46**(4):555–567, 2005. 25

[83] K Nakatani and K W Yau. **Calcium and magnesium fluxes across the plasma membrane of the toad rod outer segment.** *J Physiol*, **395**:695–729, 1988. 21

[84] J Nathans, D Thomas, and D S Hogness. **Molecular genetics of human color vision: the genes encoding blue, green, and red pigments.** *Science*, **232**(4747):193–202, 1986. 4

[85] John G. Nicholls, A. Robert Martin, Bruce G. Wallace, and Paul A. Fuchs. *From Neuron to Brain, Fourth ed.* Sinauer Associates, Inc. - Massachusetts, U.S.A., 2001. 9

[86] S Nikonov, N Engheta, and E N Jr Pugh. **Kinetics of recovery of the dark-adapted salamander rod photoresponse.** *J Gen Physiol*, **111**(1):7–37, 1998. 23, 63

[87] S Nikonov, T D Lamb, and E N Jr Pugh. **The role of steady phosphodiesterase activity in the kinetics and sensitivity of the light-adapted salamander rod photoresponse.** *J Gen Physiol*, **116**(6):795–824, 2000. 23, 63

[88] Koji M Nishiguchi, Michael A Sandberg, Aart C Kooijman, Kirill A Martemyanov, Jan W R Pott, Stephanie A Hagstrom, Vadim Y Arshavsky, Eliot L Berson, and Thaddeus P Dryja. **Defects in RGS9 or its anchor protein R9AP in patients with slow photoreceptor deactivation.** *Nature*, **427**(6969):75–78, 2004. 20

[89] H Ohguro, J P Van Hooser, A H Milam, and K Palczewski. **Rhodopsin phosphorylation and dephosphorylation in vivo.** *J Biol Chem*, **270**(24):14259–14262, 1995. 18

[90] K Palczewski. **Structure and functions of arrestins.** *Protein Sci*, **3**(9):1355–1361, 1994. 19

[91] K Palczewski. **GTP-binding-protein-coupled receptor kinases–two mechanistic models.** *Eur J Biochem*, **248**(2):261–269, 1997. 18

[92] K Palczewski, J Buczylko, H Ohguro, R S Annan, S A Carr, J W Crabb, M W Kaplan, R S Johnson, and K A Walsh. **Characterization of a truncated form of arrestin isolated from bovine rod outer segments.** *Protein Sci*, **3**(2):314–324, 1994. 19, 48

[93] K Palczewski, T Kumasaka, T Hori, C A Behnke, H Motoshima, B A Fox, I Le Trong, D C Teller, T Okada, R E Stenkamp, M Yamamoto, and M Miyano. **Crystal structure of rhodopsin: A G protein-coupled receptor.** *Science*, **289**(5480):739–745, 2000. 10

[94] K Palczewski, A S Polans, W Baehr, and J B Ames. **Ca(2+)-binding proteins in the retina: structure, function, and the etiology of human visual diseases.** *Bioessays*, **22**(4):337–350, 2000. 65

[95] K Palczewski, I Subbaraya, W A Gorczyca, B S Helekar, C C Ruiz, H Ohguro, J Huang, X Zhao, J W Crabb, and R S Johnson. **Molecular cloning and characterization of retinal photoreceptor guanylyl cyclase-activating protein.** *Neuron*, **13**(2):395–404, 1994. 21

[96] Krzysztof Palczewski, Izabela Sokal, and Wolfgang Baehr. **Guanylate cyclase-activating proteins: structure, function, and diversity.** *Biochem Biophys Res Commun*, **322**(4):1123–1130, 2004. 21, 22, 44, 63

[97] M W Pfaffl. **A new mathematical model for relative quantification in real-time RT-PCR.** *Nucleic Acids Res*, **29**(9):e45, 2001. 31

[98] N J Philp, W Chang, and K Long. **Light-stimulated protein movement in rod photoreceptor cells of the rat retina.** *FEBS Lett*, **225**(1-2):127–132, 1987. 25

[99] E N Jr Pugh, T Duda, A Sitaramayya, and R K Sharma. **Photoreceptor guanylate cyclases: a review.** *Biosci Rep*, **17**(5):429–473, 1997. 20, 65

[100] E N Jr Pugh, S Nikonov, and T D Lamb. **Molecular mechanisms of vertebrate photoreceptor light adaptation.** *Curr Opin Neurobiol*, **9**(4):410–418, 1999. 66

[101] E.N. Pugh and T.D. Lamb. *Phototransduction in Vertebrate Rods and Cones: Molecular Mechanisms of Amplification, Recovery and Light Adaptation.* Elsevier Science, 2000. 14, 15, 17, 65

[102] A Pulvermuller, D Maretzki, M Rudnicka-Nawrot, W C Smith, K Palczewski, and K P Hofmann. **Functional differences in the interaction of arrestin and its splice variant, p44, with rhodopsin.** *Biochemistry*, **36**(30):9253–9260, 1997. 19, 48

[103] Boris Reidel, Wilda Orisme, Tobias Goldmann, W Clay Smith, and Uwe Wolfrum. **Photoreceptor vitality in organotypic cultures of mature vertebrate retinas validated by light-dependent molecular movements.** *Vision Res*, **46**(27):4464–4471, 2006. 28, 30, 51, 64

[104] Shannon M Saszik, John G Robson, and Laura J Frishman. **The scotopic threshold response of the dark-adapted electroretinogram of the mouse.** *J Physiol*, **543**(Pt 3):899–916, 2002. 51

[105] E A Schwartz. **Depolarization without calcium can release gamma-aminobutyric acid from a retinal neuron.** *Science*, **238**(4825):350–355, 1987. 6

[106] T Shinohara, B Dietzschold, C M Craft, G Wistow, J J Early, L A Donoso, J Horwitz, and R Tao. **Primary and secondary structure of bovine retinal S antigen (48-kDa protein).** *Proc Natl Acad Sci U S A*, **84**(20):6975–6979, 1987. 19

[107] A K Singh, G Kumar, T Shinohara, and H Shichi. **Porcine S-antigen: cDNA sequence and expression in retina, ciliary epithelium and iris.** *Exp Eye Res*, **62**(3):299–308, 1996. 19

[108] D P Smith, B H Shieh, and C S Zuker. **Isolation and structure of an arrestin gene from Drosophila.** *Proc Natl Acad Sci U S A*, **87**(3):1003–1007, 1990. 19

[109] W C Smith, A H Milam, D Dugger, A Arendt, P A Hargrave, and K Palczewski. **A splice variant of arrestin. Molecular cloning and localization in bovine retina.** *J Biol Chem*, **269**(22):15407–15410, 1994. 19

[110] Maxim Sokolov, Arkady L Lyubarsky, Katherine J Strissel, Andrey B Savchenko, Viktor I Govardovskii, Edward N Jr Pugh, and Vadim Y Arshavsky. **Massive light-driven translocation of transducin between the two major compartments of rod cells: a novel mechanism of light adaptation.** *Neuron*, **34**(1):95–106, 2002. 25, 26, 63

[111] P. Sterling. *Retina. In The Synaptic Organization of the Brain, Fourth ed.* New York: Oxford Univ. Press., 1997. 8

[112] Kai-Florian Storch, Carlos Paz, James Signorovitch, Elio Raviola, Basil Pawlyk, Tiansen Li, and Charles J Weitz. **Intrinsic circadian clock of the mammalian retina: importance for retinal processing of visual information.** *Cell*, **130**(4):730–741, 2007. 34

[113] E Strettoi and R H Masland. **The number of unidentified amacrine cells in the mammalian retina.** *Proc Natl Acad Sci U S A*, **93**(25):14906–14911, 1996. 8

[114] Katherine J Strissel, Polina V Lishko, Lynn H Trieu, Matthew J Kennedy, James B Hurley, and Vadim Y Arshavsky. **Recoverin undergoes light-dependent intracellular translocation in rod photoreceptors.** *J Biol Chem*, **280**(32):29250–29255, 2005. 26

[115] Katherine J Strissel, Maxim Sokolov, Lynn H Trieu, and Vadim Y Arshavsky. **Arrestin translocation is induced at a critical threshold of visual signaling and is superstoichiometric to bleached rhodopsin.** *J Neurosci*, **26**(4):1146–1153, 2006. 25, 26, 48, 51

[116] Tatiana Subkhankulova and Frederick J Livesey. **Comparative evaluation of linear and exponential amplification techniques for expression profiling at the single-cell level.** *Genome Biol*, **7**(3):R18, 2006. 28, 41

[117] A Surguchov, J D Bronson, P Banerjee, J A Knowles, C Ruiz, I Subbaraya, K Palczewski, and W Baehr. **The human GCAP1 and GCAP2 genes are arranged in a tail-to-tail array on the short arm of chromosome 6 (p21.1).** *Genomics*, **39**(3):312–322, 1997. 21

[118] M Tachibana and T Okada. **Release of endogenous excitatory amino acids from ON-type bipolar cells isolated from the goldfish retina.** *J Neurosci*, **11**(7):2199–2208, 1991. 7

[119] A M Timmers, B R Newton, and W W Hauswirth. **Synthesis and stability of retinal photoreceptor mRNAs are coordinately regulated during bovine fetal development.** *Exp Eye Res*, **56**(3):257–265, 1993. 19

[120] V Torre, H R Matthews, and T D Lamb. **Role of calcium in regulating the cyclic GMP cascade of phototransduction in retinal rods.** *Proc Natl Acad Sci U S A*, **83**(18):7109–7113, 1986. 22, 63, 66

[121] M Tsuda, M Syed, K Bugra, J P Whelan, J F McGinnis, and T Shinohara. **Structural analysis of mouse S-antigen.** *Gene*, **73**(1):11–20, 1988. 19

[122] S A Vishnivetskiy, C Schubert, G C Climaco, Y V Gurevich, M G Velez, and V V Gurevich. **An additional phosphate-binding element in arrestin molecule. Implications for the mechanism of arrestin activation.** *J Biol Chem*, **275**(52):41049–41057, 2000. 64

[123] James M Wettenhall and Gordon K Smyth. **limmaGUI: a graphical user interface for linear modeling of microarray data.** *Bioinformatics*, **20**(18):3705–3706, 2004. 28

[124] J P Whelan and J F McGinnis. **Light-dependent subcellular movement of photoreceptor proteins.** *J Neurosci Res*, **20**(2):263–270, 1988. 25

[125] U Wilden. **Duration and amplitude of the light-induced cGMP hydrolysis in vertebrate photoreceptors are regulated by multiple phosphorylation of rhodopsin and by arrestin binding.** *Biochemistry*, **34**(4):1446–1454, 1995. 18

[126] U Wilden, S W Hall, and H Kuhn. **Phosphodiesterase activation by photoexcited rhodopsin is quenched when rhodopsin is phosphorylated and binds the intrinsic 48-kDa protein of rod outer segments.** *Proc Natl Acad Sci U S A*, **83**(5):1174–1178, 1986. 10, 18

[127] S E Wilkie, R J Newbold, E Deery, C E Walker, I Stinton, V Ramamurthy, J B Hurley, S S Bhattacharya, M J Warren, and D M Hunt. **Functional characterization of missense mutations at codon 838 in retinal guanylate cyclase correlates with disease severity in patients with autosomal dominant cone-rod dystrophy.** *Hum Mol Genet*, **9**(20):3065–3073, 2000. 65

[128] J Xu, R L Dodd, C L Makino, M I Simon, D A Baylor, and J Chen. **Prolonged photoresponses in transgenic mouse rods lacking arrestin.** *Nature*, **389**(6650):505–509, 1997. 19, 64

[129] Xiangmin Xu, A B Bonds, and Vivien A Casagrande. **Modeling receptive-field structure of koniocellular, magnocellular, and parvocellular LGN cells in the owl monkey (Aotus trivigatus).** *Vis Neurosci*, **19**(6):703–711, 2002. 9

[130] T Yamada, Y Takeuchi, N Komori, H Kobayashi, Y Sakai, Y Hotta, and H Matsumoto. **A 49-kilodalton phosphoprotein in the Drosophila photoreceptor is an arrestin homolog.** *Science*, **248**(4954):483–486, 1990. 19

[131] A Yamazaki, P J Stein, N Chernoff, and M W Bitensky. **Activation mechanism of rod outer segment cyclic GMP phosphodiesterase. Release of inhibitor by the GTP/GTP-binding protein.** *J Biol Chem*, **258**(13):8188–8194, 1983. 15

[132] R W Young. **The renewal of photoreceptor cell outer segments.** *J Cell Biol*, **33**(1):61–72, 1967. 5

[133] Joshua S Yuan, Ann Reed, Feng Chen, and C Neal Jr Stewart. **Statistical analysis of real-time PCR data.** *BMC Bioinformatics*, **7**:85, 2006. 31

# Acknowledgements

...